

Article

Adaptable Monitoring Package Development and Deployment: Lessons Learned for Integrated Instrumentation at Marine Energy Sites

Brian Polagye^{1,*}, James Joslin², Paul Murphy¹, Emma Cotter^{1,3}, Mitchell Scott², Paul Gibbs², Christopher Bassett² and Andrew Stewart¹

¹ University of Washington, Department of Mechanical Engineering, Seattle, WA 98195; bpolagye@uw.edu (B.P.), pgmurphy@uw.edu (P.M.)

² University of Washington, Applied Physics Laboratory, Seattle, WA 98105; jbjoslin@uw.edu (J.J.), miscott@uw.edu (M.S.), gibbsp@uw.edu (P.G.), cbassett@uw.edu (C.B.), arstew@uw.edu (A.S.)

³ Woods Hole Oceanographic Institution, Woods Hole, MA 02543; ecotter@whoi.edu (E.C.)

* Correspondence: bpolagye@uw.edu

Version July 9, 2020 submitted to *J. Mar. Sci. Eng.*

Abstract: Integrated instrumentation packages are an attractive option for environmental and ecological monitoring at marine energy sites, as they can support a range of sensors in a form factor compact enough for the operational constraints posed by energetic waves and currents. Here we present details of the architecture and performance for one such system - the Adaptable Monitoring Package - which supports active acoustic, passive acoustic, and optical sensing to quantify the physical environment and animal presence at marine energy sites. We describe cabled and autonomous deployments and contrast the relatively limited system capabilities in an autonomous operating mode with more expansive capabilities, including real-time data processing, afforded by shore power or in-situ power harvesting from waves. Across these deployments, we describe sensor performance, outcomes for biological target classification algorithms using data from multibeam sonars and optical cameras, and the effectiveness of measures to limit biofouling and corrosion. On the basis of these experiences, we discuss the evidenced requirements for integrated instrumentation, possible operational concepts for monitoring the environmental and ecological effects of marine energy converters using such systems, and the engineering trade-offs inherent in their development. Overall, we find that integrated instrumentation can provide powerful capabilities for observing rare events, managing the volume of data collected, and mitigating potential bias to marine animal behavior. These capabilities may be as relevant to the broader oceanographic community as they are to the emerging marine energy sector.

Keywords: environmental monitoring; integrated instrumentation; marine renewable energy

1. Introduction

The conversion of marine energy resources (e.g., waves, currents) to electricity is at an early stage of development and, as a consequence of scientific and regulatory uncertainty, studies of environmental¹ effects have been a priority for initial deployments [1,2]. By understanding these effects during the formative stages of marine energy technology development, it may be possible to mitigate undesirable environmental impacts during scale-up to large arrays of wave energy converters

¹ Throughout, we use “environmental” as a shorthand for physical (e.g., current velocity) and ecological (e.g., animal presence) attributes.

26 or current turbines. However, such studies are complicated by the energetic environments at marine
27 energy sites, which are at oceanographic extremes. These conditions degrade remote sensing and pose
28 challenges for instrumentation deployment, operation, recovery, and survival.

29 At wave energy sites, average annual energy fluxes often exceed 30 kW/m of linear wave crest
30 [3], implying significant wave heights greater than several meters during much of the year. To
31 date, wave energy developments have taken place in water depths less than 100 m, such that wave
32 orbital velocities are appreciable (e.g., > 1 m/s) over much of the water column during extreme
33 events [4]. For river and ocean currents, developments have focused on locations where currents
34 continuously exceed 1 m/s [5]. For tidal currents, peak currents can exceed 4 m/s [6–8]. Tidal and
35 river current sites are typically scoured to pebbles, cobbles, or bedrock and near-bed currents can be
36 sufficient to intermittently mobilize the seabed [9]. Water depth at sites of commercial interest are
37 also generally less than 100 m. These conditions, in combination with the relatively broad range of
38 potential environmental interactions, have motivated the development of integrated instrumentation
39 systems that can minimize vessel operations and ensure system reliability for multi-month studies.

40 The potential benefit from integrating a broad range of instrumentation in relatively compact
41 systems has been recognized by the marine energy research community since at least 2014 [10] and
42 several integrated systems have been developed and deployed for marine energy environmental
43 research in recent years. These include the Adaptable Monitoring Package (AMP), which is the focus
44 of this paper, the Fundy Advanced Sensor Technology (FAST) platform developed by the Fundy
45 Ocean Research Centre for Energy (FORCE) [11], the Flow and Benthic Ecology (FLOWBEC) platform
46 developed by the University of Aberdeen [12], the Integrated Monitoring Package developed by the
47 European Marine Energy Centre [11], and “Plug & Play” under development by the Sea Mammal
48 Research Unit at St. Andrews University [11]. Each system accommodates a range of sensors, including:

- 49 • Passive acoustics: broadband hydrophones, fish tag receivers²;
- 50 • Active acoustics: multibeam sonars, echosounders, acoustic Doppler current profilers; and
- 51 • Optical cameras: high definition machine vision, including artificial illumination.

52 We emphasize the importance of prioritized monitoring requirements that address the unique
53 and challenging aspects of conducting environmental observations at marine energy sites. First,
54 observations should not bias animal behavior. This can occur due to emitted sound from active sonars
55 [13,14] or artificial illumination [15,16]. Second, it is desirable to capture “rare events”³, since events
56 with a low probability of occurrence but potentially severe consequence (e.g., marine mammal collision
57 with a current turbine) are of regulatory concern [1,2]. Third, the volume of data must be manageable to
58 avoid impeding timely analysis and insight [18]. We note that the first and third monitoring priorities
59 are in apparent conflict with the second, as continuous observation is required to capture rare events
60 [19], but continuous observation elevates the risk of biasing animal behavior and, if all observations
61 are archived, can generate unmanageable volumes of data.

62 These priorities, in combination with the types of sensors needed to study interactions of interest
63 and site characteristics, motivate the following deviations from traditional oceanographic practices:

- 64 • Power demands for individual sensors can be relatively high (i.e., > 100 W), which are more in
65 line with cabled observatories [20] than autonomous sensor platforms [21,22];

² Specialized hydrophones that continuously monitor for unique identifiers that are acoustically broadcast by tags attached to or implanted in fish.

³ Here, we define “rare events” as observations of marine animals that are infrequently present in a continuous time series. Depending on the monitoring objectives for a specific study at a marine energy site, the definition of “rarity” might be construed as particular predator-prey interactions (i.e., combinations of animal presence) or relatively infrequent behaviors for relatively common marine animals. Alternatively, extreme value analysis can provide a more objective definition of rarity (e.g., [17]).

- 66 • Because data rates for some sensors are relatively high (i.e., > 1 Gbps), automatic processing and
67 filtering of collected data are necessary to avoid accruing an unmanageable volume of data (i.e.,
68 discarding data that are not of specific interest between acquisition and archival)⁴;
- 69 • Deployment, maintenance, and recovery operations for instrumentation must be compatible with
70 marine energy site characteristics (weather and current windows, depth); and
- 71 • Systems must be able to operate effectively in waves and currents conducive to marine energy
72 generation.

73 A variety of design trade-offs are encountered when integrating instrumentation. While some
74 of these overlap with other areas of oceanographic observation, such as cabled observatories, that
75 experience has not generally been translated to the archival literature. Consequently, developers of
76 integrated instrumentation for marine energy applications have faced broad uncertainties, including:

- 77 • What are the functional ranges and detection capabilities for sensors when deployed in the
78 energetic environments at marine energy sites?
- 79 • What is the risk of individual sensors interfering with each other when combined in a single
80 package?
- 81 • What are the benefits of including multiple types of sensors on the same package?
- 82 • Can automatic target detection and classification reduce the volume of data produced by
83 continuous observation?
- 84 • Is integrated instrumentation reliable enough to be incorporated into monitoring plans for
85 permitting/consenting of marine energy projects?
- 86 • How much mitigation effort should be expended to prevent corrosion and biofouling?

87 While these questions cannot be answered by an individual deployment, trends do become apparent
88 when experience spans multiple deployments. The primary objective of this paper is, on the basis of
89 our aggregate experience, to provide some answers to these, and other, questions about the strengths
90 and weaknesses of integrated instrumentation in a marine energy context. Section 2 provides details
91 of the AMP architecture's hardware and software, as well as the rationale in design decisions. We then
92 describe four representative deployments in Section 3 with contrasting configurations and operational
93 strategies. In Section 4, we generalize system and sensor performance, as well as describe progress
94 towards automatic target classification. Outcomes and lessons learned from detection and classification
95 algorithms are summarized here, with more comprehensive treatment in separate publications [19,23,
96 24]. On the basis of these deployments, in Section 5, we discuss evidenced requirements for successful
97 utilization of integrated instrumentation, operational concepts for implementation, and cost-benefit
98 considerations for integration.

99 2. System Architecture

100 At a high level, the AMP has three subsystems: the package of integrated sensors, an external
101 power source, and a control computer. Some elements are deployment-agnostic (e.g., integration
102 hub), while other elements (e.g., sensors) are specific to a deployment. As shown in Figure 1, power
103 demands and bi-directional communications for individual sensors are aggregated at an integration
104 hub, which receives power from a single source and distributes this to several direct current (DC)
105 buses for use by instruments. Because data rates exceed 1 Gbps and the distance between the hub and
106 control computer can exceed 1 km, the backbone communication between the integrated sensors and

⁴ This is common practice for some autonomous sensors. For example, one passive acoustic sensor for quantifying cetacean presence-absence, the C-POD-F (Chelonia Ltd., U.K.) continuously monitors frequencies between 20 kHz and 160 kHz by sampling at 1 MHz, but processes the data in real-time to identify candidate echolocation clicks and archives only statistical information about those clicks for post-recovery analysis. Similar principles apply to fish tag receivers. The Vemco VR2W (Innovasea, U.S.) continuously monitors for tags with a transmit frequency of 69 kHz, but only stores the time and unique tag identifier of decoded detections.

107 control computer is by fiber optic media conversion⁵. The control computer provides several functions:
 108 configuring individual sensors, holding temporary data from all sensors in memory, processing these
 109 data in real time, and archiving data when targets of interest are detected.

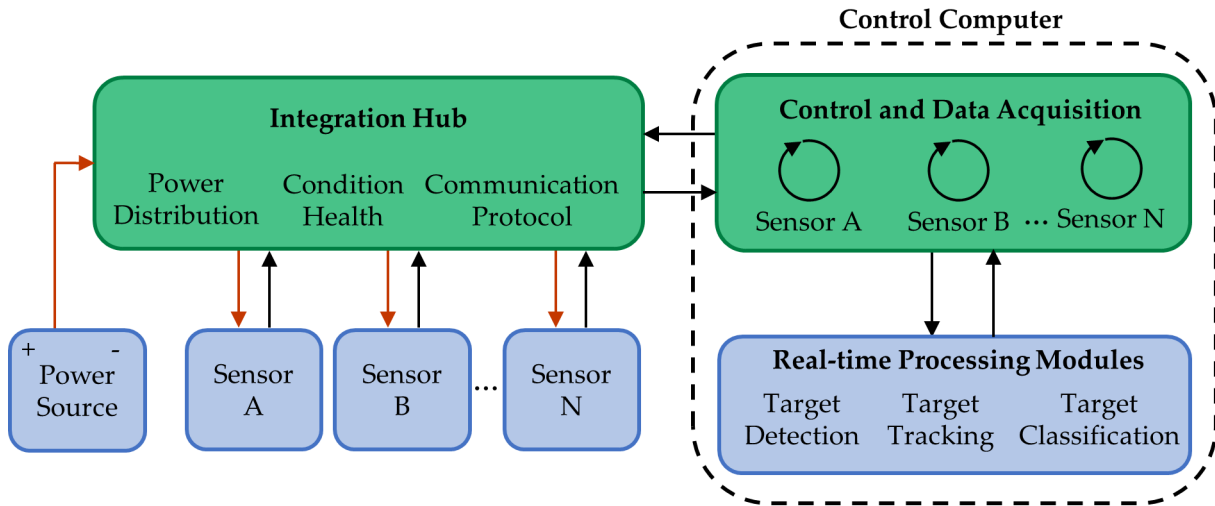


Figure 1. AMP architecture schematic. Black arrows denote flows of data, red arrows denote flows of power, and shading differentiates between deployment-specific (blue) and deployment-agnostic (green) components.

110 The following sections describe the integration hub, individual sensors, and software architecture
 111 in more detail.

112 2.1. Integration Hub

113 At the core of the AMP is the power and data integration hub. The hub aggregates data streams
 114 from connected sensors, converts these to Ethernet protocol, if necessary (e.g., serial to Ethernet
 115 conversion), and converts from copper to fiber media for transmission over an umbilical. This link is
 116 bi-directional and allows the control computer to adjust sensor configuration during deployment. The
 117 hub monitors the current draw on each output channel to detect spikes that could indicate a sensor
 118 malfunction. Similarly, the hub contains temperature and humidity sensors, as well as an inertial
 119 measurement unit. Finally, the hub generates analog trigger signals for each active sonar to prevent
 120 acoustic interference across channels (i.e., “cross-talk”).

121 The hub uses custom electronics to distribute DC voltage at two input levels, 200-400 VDC
 122 or 48 VDC⁶, to sensors with nominal inputs of 48, 24, 12, or 5 VDC. There are 10 instrument
 123 ports on the integration hub that can be electrically isolated (e.g., in the event of a ground fault)
 124 by double-pull/double-throw relays for power and opto-isolated communication lines. However,
 125 the integration hub can support more than 10 sensors by aggregating multiple sensors to a single
 126 instrument port (e.g., a hydrophone array using only one instrument port on the hub).

127 Key component specifications are summarized in Table 1. The power draw for these “hotel” loads
 128 is approximately 30 W. Power conversion efficiency depends on the instantaneous sensor loads and
 129 supply voltage, but has generally been above 90 %.

⁵ The maximum distance is limited by fiber optic signal attenuation, approximately 40 km with existing hardware.

⁶ These two voltage input levels accommodate battery power proximate to the sensors (48 VDC), as well as power transmission over a shore cable (200-400 VDC).

Table 1. Key integration hub components.

Component function	Manufacturer	Model(s)
DC-DC power conversion	Vicor	DCM 200-400 VDC, DCM 48 – 48 VDC, Mini 48-24 VDC, Mini 48-12 VDC
Media conversion	Moxa	EDS-G516E Series
Serial to Ethernet conversion	Moxa	NPort-5200 Series

130 2.2. Mechanical Components

131 Considerations for mechanical integration include site, deployment, and operational constraints.
 132 Impact design factors include access to cables during assembly, sensor field of view orientation, and
 133 minimization of structural loading from hydrodynamic drag (e.g., compact form factor, fairings). The
 134 integration hub and subsystems that are not already in submersible housings (e.g., optical cameras)
 135 are contained in custom cylindrical pressure housings (depth rating of 200 m). If heat dissipation
 136 is required, the housings are anodized aluminum tube, otherwise lower-cost schedule 80 PVC is
 137 used. Housing endcaps are secured with a filament and sealed with double piston O-rings. Wherever
 138 possible, plastics (e.g., homopolymer acetal, PVC) are used to electrically isolate components and
 139 eliminate corrosion from dissimilar metal contact. Depending on the target design life of the platform,
 140 fastening hardware is selected from either all-coat mild steel, 316 stainless steel, silicon bronze, or
 141 titanium. In addition, structural components critical to the deployment and recovery operations
 142 include redundant hardware in case of unexpected corrosion.

143 2.3. Sensor Hardware

144 As summarized in Table 2, multiple sensors have been integrated with the AMP architecture,
 145 though not all of these sensors have been deployed simultaneously on a single AMP. With the exception
 146 of the optical cameras, which involved a custom solution for stereo imaging and strobe illumination,
 147 commercial instrumentation was integrated with limited modification (e.g., the Simrad WBTmini
 148 transceiver required a custom pressure housing). The fields of view for optical and acoustic instruments
 149 are shown schematically in Figure 2. The depth rating varies by sensor from a minimum of 20 m for
 150 the echosounder transducer to a maximum of 4000 m for the Tritech and Kongsberg multibeam sonars.

Table 2. AMP sensors

Category	Sensor	Input voltage [VDC]	Maximum acquisition rate (stand-alone / AMP synchronized) [Hz]	Power requirement (synchronized acquisition rate) [W]	Data rate (single instrument)	Comm protocol	Field of view	Maximum range [m]
Acoustic Doppler current profiler	Nortek Signature 500 (Norway)	12-48	8/5	23	$< 3 \times 10^{-4a}$	RS-232 or Ethernet	2.9° beam width	70
	BlueView M900-2250 (U.S.)	12-48	15/10	19.2	< 0.1 MB/frame ^b < 0.1 MB/frame ^{cd}	Ethernet	130x20° swath 130x20° swath 120° <i>irc</i> x swath	200 kHz: 10 900 kHz: 100
Multibeam sonar	Tritech Gemini (U.K.)	19-72	97/19	16-27	< 1.3 MB/frame	Ethernet	3,7,15, or 30° swath	120
	Kongsberg M3 (Norway)	12-36	40/10	24.0	< 0.001 MB/message 3×10^{-6} MB/sample	Ethernet	18° beam width	38 kHz: > 500 200 kHz: 200 > 100
Echosounder	Simrad WB7mini (w/ 38/200 kHz combi-transducer) (Norway)	12-16	38 kHz: $< 4 / < 4$ 200 kHz: $> 10 / 10$ Passive: $> 10 / 10$	38 kHz: 6 200 kHz: 3 Passive: 2	0.002 MB/ping ^e	Ethernet	18° beam width	38 kHz: > 500 200 kHz: 200 > 100
	Vemco VR2C (Canada)	10-32	N/A	0.2	< 0.001 MB/message 3×10^{-6} MB/sample	RS-232	Omni-directional	N/A
Passive acoustic	icListen HF (Ocean Sonics, Canada)	24	512,000/512,000	3.6	3×10^{-6} MB/sample	Ethernet	N/A	N/A
	SeaBird ecoBB (650 nm) (U.S.)	7-15	8	< 1	3×10^{-6} MB/sample	RS-232	N/A	N/A
Optical camera	Allied Vision Manta G201b & G507b (Canada)	12	23/10	4.8	< 0.3 MB/frame ^f	Ethernet	65x56°	0-30
Xenon strobe	Excelitas MVS-500 (U.S.)	12	14/10	63.6	N/A	N/A	N/A	N/A
LED strobe (red/white)	Custom LED Arrays	48	Continuous/camera-limited	49	N/A	N/A	N/A	N/A

^a At configured resolution of 0.5 m and range of 8 m (MSL-1 and MSL-2 deployments)^b Compressed JPEG image format in polar coordinates (range and transducer agnostic)^c Compressed JPEG image format in Cartesian coordinates (range and transducer agnostic)^d ASCII format with arc resolution of 0.95o (15 o vertical beam angle), range resolution of 0.03 m, and range of 50 m (MSL-1 and WAMP deployments)^e Single operational channel logging to a range of 75 m with the smallest file configuration (narrowband operation with high data compression). The data rate is sensitive to signal types (broadband vs. narrowband), data compression options, and logging range [25]. The use of broadband signals with minimal compression increases the data rate by approximately two orders of magnitude.^f Compressed JPEG from 8-bit, monochrome image (5Mpx from G507b)

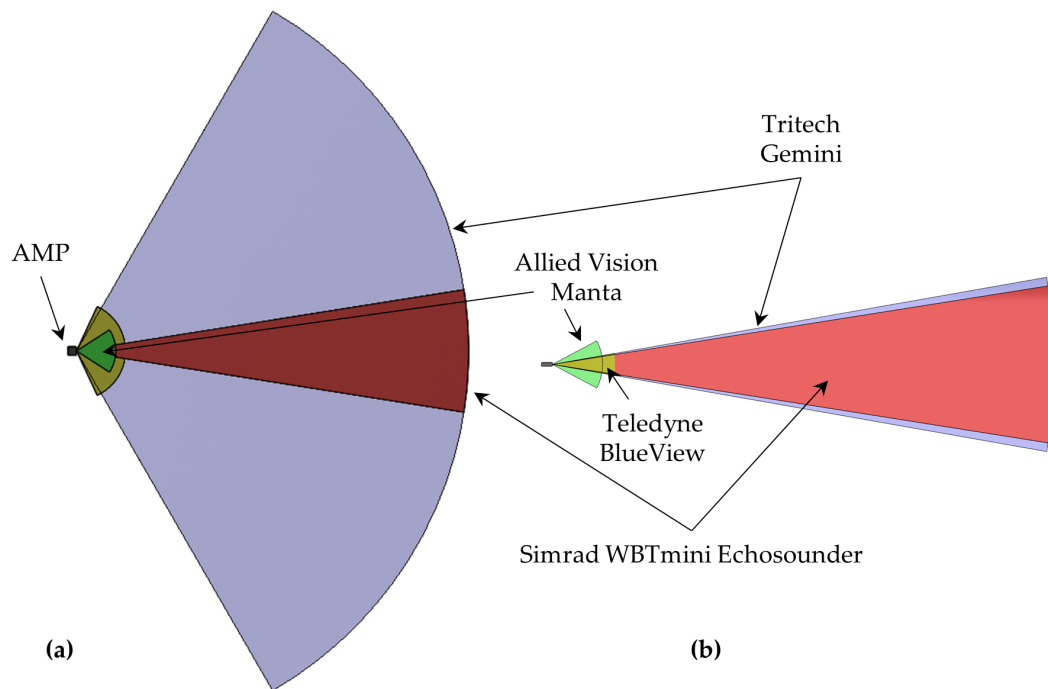


Figure 2. AMP sensor field of view for a horizontally-oriented deployment showing the AMP body to scale for (a) top-view and (b) side-view with the Manta optical cameras to 8 m (nominal range), BlueView sonar to 10 m, Gemini sonar to 80 m, and Simrad echosounder to 80 m.

151 Some of the sensors have geometric constraints that drove design decisions. The passive acoustic
 152 sensors (fish tag receiver and hydrophones) are ideally located away from obstructions. Further,
 153 maximizing the localizing hydrophone array's baseline extends the practical bandwidth to lower
 154 frequencies and can increase location resolution and accuracy [26,27]. For stereo-optical cameras with a
 155 target range less than 10 m, baseline separation between the cameras of at least 0.4 m is recommended,
 156 as is a camera-light separation of 0.4 m to limit optical backscatter [28,29]. These requirements motivate
 157 larger physical dimensions, which conflicts with the operational challenges of working at a marine
 158 energy site that motivate the most compact arrangement possible.

159 2.4. Sensor Software

160 The AMP control software is written in LabVIEW (National Instruments) and provides users
 161 with a graphical user interface (GUI) for direct control of the AMP. The software acquires data, as well
 162 as controls the AMP's main electronics bottle and individual sensors. The software is composed of
 163 interconnected LabVIEW "virtual instruments" (VIs), running in parallel. A core module handles
 164 communications with the integration hub to toggle power to individual sensors, observe system health
 165 sensors (e.g., current draw) and, in the event that normal thresholds are exceeded, automatically
 166 disable affected systems. This modular software structure allows a variety of real-time processing
 167 codes to be used to control data acquisition and for the sensor mix to be tailored to the requirements of
 168 a particular deployment.

169 Each sensor is operated by an individual VI that handles configuration (e.g., gain, range for a
 170 multibeam sonar) and parses the data stream. The specific implementation varies by sensor. Many
 171 sensor manufacturers provide application programming interfaces (APIs) for communication over
 172 TCP/IP or serial bus according to documented telemetry. Some APIs allow direct communication
 173 with an instrument (e.g., Ocean Sonics icListen HF), while others use an external application to
 174 mediate between LabVIEW and the instrument (e.g., Kongsberg M3, Simrad WBT Mini). The BlueView
 175 M900-2250 utilizes a .NET based software development kit (SDK) that can be accessed directly by
 176 LabVIEW, while the Tritech Gemini 720is SDK requires an intermediate software layer in C++. Data

177 from sensors with relatively low data rates (e.g., current profiler, optical backscatter) can be continually
178 archived. Data from sensors with relatively high data rates (e.g., optical camera, multibeam sonar)
179 are stored in variable-length ring buffers (typically 60 seconds) in the computer's volatile memory.
180 These ring buffers are archived when a command is generated either by a user, on a fixed duty cycle,
181 or by a real-time data-processing module. The ring buffer structure serves three purposes: 1) when an
182 archival command is generated, contextual data before the event is available in temporary storage; 2)
183 processing codes do not need to operate in true "real-time", so long as they process data before they
184 are overwritten in the ring buffer; and 3) data stored in memory can be used to establish background
185 levels for real-time target detection. Real-time processing modules are implemented in either MATLAB
186 (Mathworks) or Python and communicate with the core LabVIEW module via User Datagram Protocol.

187 *2.5. Biofouling Mitigation Measures*

188 For longer-term deployments, biofouling mitigation measures can be critical to maintaining
189 sensor operations. The optical backscatter sensor has an integrated copper shutter with a brush
190 wiper. Similarly, the optical cameras and illumination sources are equipped with mechanical
191 wipers (Zebra-Tech, Ltd. Hydro-Wiper) and copper face plates surrounding optical surfaces [30].
192 Ultraviolet (UV) lighting (AML Oceanographic) is used to minimize biofouling on transducers both
193 as a precautionary measure due to uncertainties about the impact on performance and to avoid
194 potential damage during cleaning. All biofouling control (e.g., wiper actuation) is integrated into a
195 single, custom package that interfaces with the integration hub like the other AMP sensors. For the
196 most recent deployment (Section 3.4), which included both wipers and UV lighting, the wipers were
197 actuated every 30 minutes and the UV lights were operated for 30 minutes every 60 minutes. Each
198 wiper actuation draws approximately 6.5 W for 8 s and each UV light draws 2.5 W when illuminated. In
199 addition, prior to each deployment, transducer and hydrophone elements are coated with a zinc oxide
200 paste (40 % content diaper rash cream). To reduce clean-up time following extended deployments,
201 we have adopted the practices of wrapping housings in vinyl tape and sheathing cables with plastic
202 "painter's hose". These can be easily removed (along with fouling) and disposed of at recovery.

203 *2.6. Adjustable Field of View*

204 For initial deployments, the AMP sensor field of view was fixed. In the most recent deployment
205 (Section 3.4), a tilt actuator (Remote Ocean Systems P-25) was integrated and allows the sensor head
206 (instrumented with directional sensors such as the optical cameras and active sonars) to rotate through
207 an arc of 270°.

208 **3. Representative Deployments**

209 In this section, salient details from four AMP deployments are presented in chronological order,
210 each of which demonstrates a particular capability or contrasts modes of operation (Table 3, Figure
211 3). The primary objective of these deployments was to explore the general benefit of integrated
212 instrumentation, with a secondary objective of collecting opportunistic environmental data (i.e., data
213 that could inform future studies with specific hypotheses or permitting processes).

Table 3. Adaptable Monitoring Package deployment summary. “System availability” is % of time available for sensing and “system activity” is % of time actively sensing. Power requirements are only for offshore components.

Deployment	MSL-1	AutoAMP	WAMP	MSL-2
Location	Sequim Bay, WA (MSL) 48° 4.76' N, 123° 2.68' W 10 Jan — 28 Mar 2017 (77 days) ≈90%/90%	Newport, OR (PacWave) 44° 32.86' N, 124° 13.78' W 15 Aug — 29 Sep 2017 (44 days) >99%/1.7%	Kaneoche, HI (WETS) 21°27.94' N, 157° 45.04' W 15 Oct 2018 — 28 Jan 2019 (105 days) 84%/84%	Sequim Bay, WA (MSL) 48° 4.79' N, 123° 2.60' W 30 Jan — 28 May 2019 (118 days) 96%/96%
System availability/activity				
Deployment type	Cabled bottom lander	Autonomous bottom lander	Autonomous surface platform	Cabled bottom lander
Distance to shore	0.1 km	12.5 km	1.5 km	0.2 km
Water depth	8 m (MLLW)	70 m	30 m	7 m (MLLW)
Dominant environment	Tidal current	Wave	Wave	Tidal current
Power requirement	373 W	161 W	696 W	240 W
Power source	Shore cable	Battery bank (6900 Wh capacity)	Battery-backed wave energy converter	Shore cable
Real-time processing	Multibeam sonar triggered acquisition	—	Multibeam sonar triggered acquisition	Multibeam sonar triggered acquisition and classification
Primary sensor orientation	Across-channel, fixed	Upward-looking, fixed	Downward-looking, fixed	Across-channel, variable tilt
Biofouling mitigation	Camera and strobe wipers	—	Camera and strobe wipers	Camera and strobe wipers UV lights for sonars
Optical sensors				
Cameras	Allied Vision Manta G-201b	—	Allied Vision Manta G-507b	Allied Vision Manta G-507b
Illumination	Excelitas MVS-5000	—	Custom white and red LEDs	Custom white and red LEDs
Optical backscatter	—	—	—	Seabird ecoBB
Passive acoustic sensors				
Hydrophone	OceanSonics icListen HF (4)	OceanSonics icListen HF (3)	OceanSonics icListen HF (2)	OceanSonics icListen HF (4)
Fish tag receiver	—	Vemco VR2C	—	Vemco VR2C
Active acoustic sensors				
Multibeam sonars	BlueView M900-2250 Kongsberg M3	BlueView M900-2250 Kongsberg M3	BlueView M900-2250 Kongsberg M3	BlueView M900-2250 Tritech Gemini 720is Simrad WBTmini
Echosounder	—	—	—	Nortek Signature 500
Acoustic Doppler current profiler	Nortek Signature 500	—	—	Nortek Signature 500

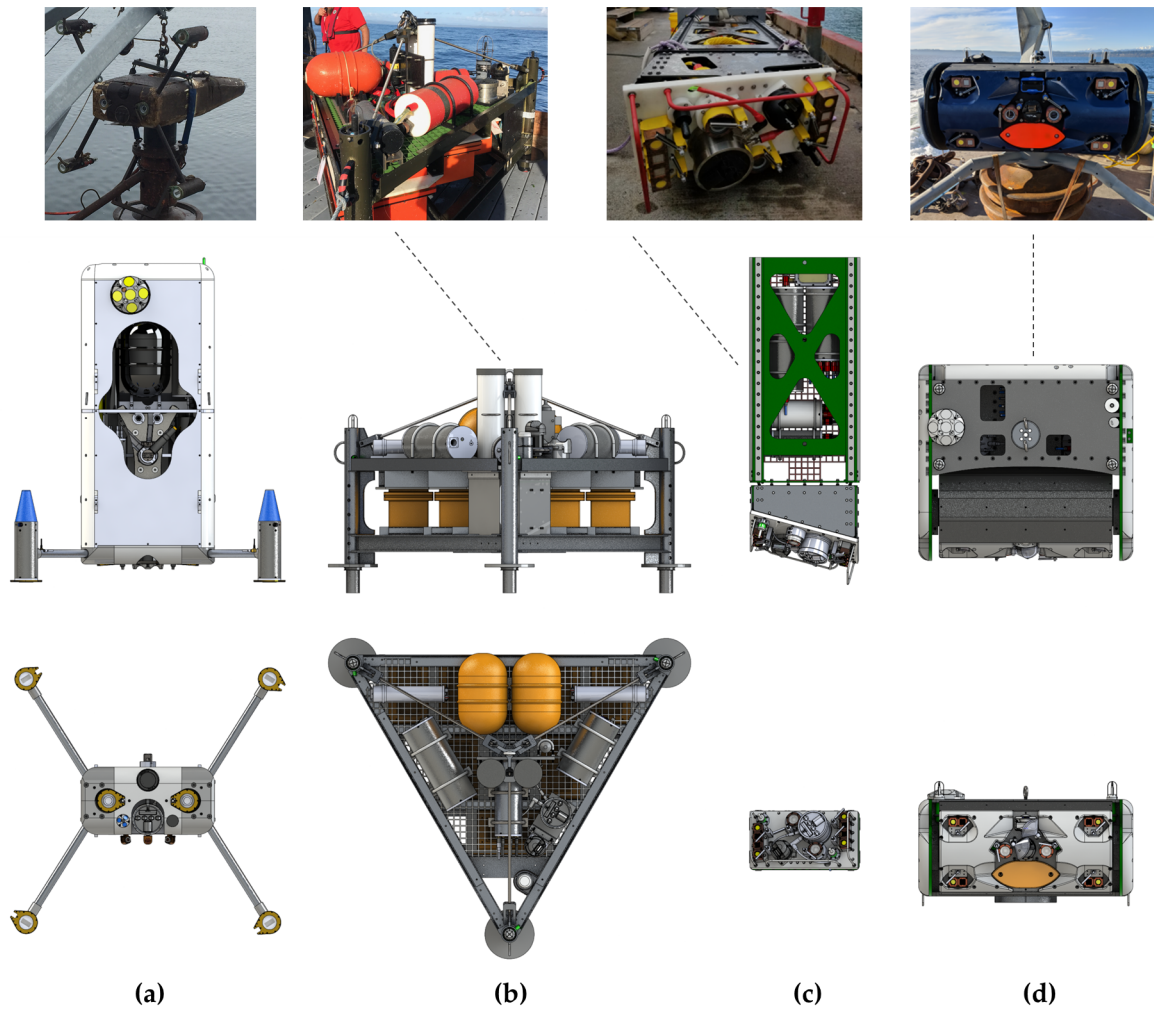


Figure 3. AMP configurations from select deployments: (a) MSL-1, (b) AutoAMP, (c) WAMP, and (d) MSL-2. Top row: Photographs of AMP configurations. Middle row: constant-scale profile view of instrumentation and core platform elements (excludes mounting structures). Bottom row: constant-scale view of primary sensor head.

214 3.1. MSL-1 Demonstration

215 During this deployment, the AMP was operated over a cable at a marine energy demonstration
 216 site, the Pacific Northwest National Laboratory’s Marine Science Lab (PNNL MSL) in Sequim, WA
 217 (Figure 4). Sensors were oriented in a horizontal plane approximately perpendicular to the direction
 218 of the tidal currents (peak velocity of ≈ 1.5 m/s). Prior deployments at PNNL MSL (not described)
 219 focused on hardware functionality and software development for individual sensors. During this
 220 deployment, for the first time, a real-time data-processing module on the shore computer detected
 221 and tracked targets in the multibeam sonar data streams (BlueView M900-2250 and Kongsberg M3)
 222 [19]. This module generated a data archival command when a tracked target exceeded apparent size
 223 and intensity thresholds⁷. Data were simultaneously collected on a sparse duty cycle to evaluate the
 224 false negative rate of the target detection and tracking module [19]. System availability (Table 3) was
 225 deemed sufficient to proceed with higher-risk, autonomous deployments.

⁷ These were manually tuned *ad hoc* to generate the maximum number of false positive detections that could be feasibly reviewed by the project team.

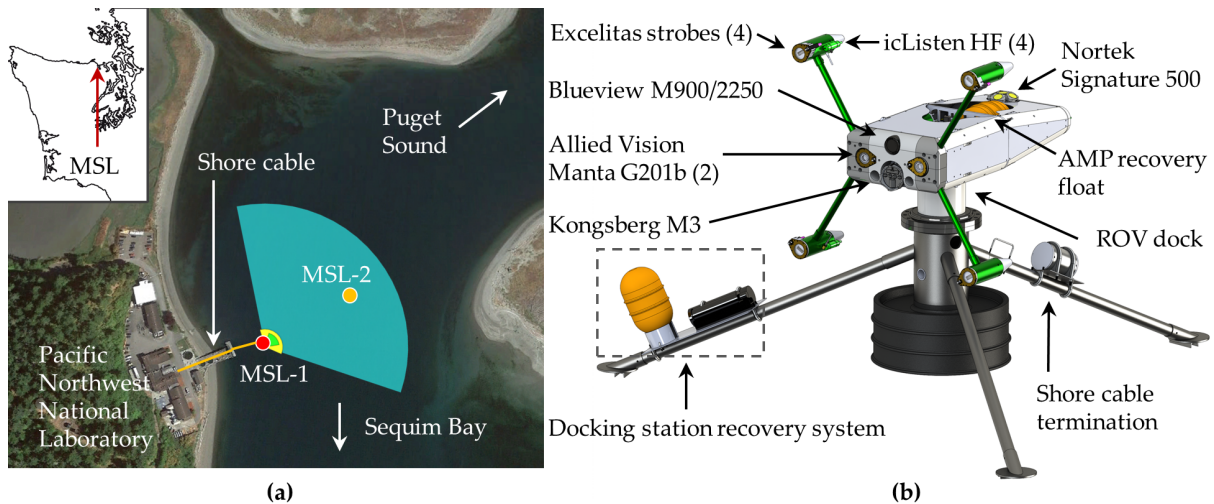


Figure 4. MSL-1 AMP deployment showing (a) site layout with MSL-2 location noted and (b) AMP and docking station lander. The AMP control computer was located on shore.

226 3.2. Autonomous Adaptable Monitoring Package (AutoAMP)

227 During this deployment, the AMP was operated autonomously using battery power in the Pacific
 228 Ocean off of Newport, OR (Figure 5). This location is under development as a grid-connected wave
 229 energy test site (PacWave South, pacwaveenergy.org) but does not yet have power or data cables back to
 230 shore. While a battery-powered system cannot meet the objectives outlined in Section 1 (i.e., continuous
 231 observation and real-time control are infeasible due to the power required), such deployments can
 232 collect useful environmental information for site development and permitting activities without
 233 incurring the expense of cable installation. Due to the water depth and moderate wave climate, the
 234 AMP only experienced significant structural loading during deployment and recovery. The battery
 235 bank (8x Deep Sea Power & Light Sea Battery modules) had a capacity of 6900 Wh and data acquisition
 236 was controlled by a compact computer (Intel NUC NUC6i7KYK) on the platform⁸. The system was
 237 operated on a duty cycle by a low-power microcontroller, acquiring 120 s of data every 2 hours. Prior
 238 to each acquisition sequence, 60 s were allocated to boot up and initialize and, following acquisition,
 239 up to 60 s to shut down. This duty cycle balanced available battery power and storage capacity (2
 240 TB) for the anticipated deployment duration. In addition, the system was configured to power on
 241 and acquire data upon detection of a tagged fish. This was achieved by passing messages from a
 242 fish tag receiver (Vemco VR2C) to the microcontroller and enabling power if a tag was detected. In
 243 doing so, the AMP could gather contextual environmental information concurrent with the presence
 244 of a tagged fish. In contrast to MSL-1, the hardware frame was configured as a bottom lander with
 245 vertically-oriented instrument and ballast provided by the battery bank.

⁸ This computer had sufficient processing power to record data streams on a duty cycle, but would not have been able to run target detection algorithms utilized during the MSL-1 deployment even if we had not been energy constrained by the batteries.

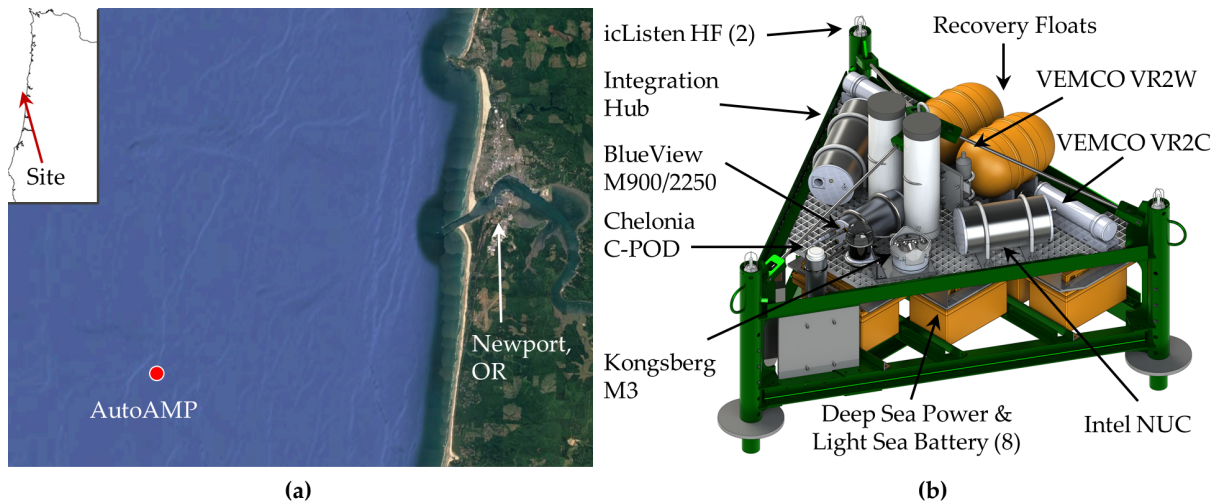


Figure 5. AutoAMP deployment showing (a) site layout and (b) AMP lander.

246 This deployment did not include optical cameras due to power limitations that prevented the use
 247 of artificial lighting to illuminate the scene (a requirement for optical cameras at this depth). Further,
 248 due to concerns about acoustic interference, a current profiler was not included⁹. These omissions
 249 prohibited optical review of targets or determination of target motion relative to currents.

250 The system operated as intended for the deployment, with the exception of two missed cycles
 251 (out of a total of 577 planned cycles) and one 24-hour period early in the deployment during which
 252 sensors recorded only 20-30 s of data before shutting down. Neither of these failure modes occurred
 253 during dockside testing prior to deployment, nor could they be replicated in the lab *post hoc*. For each
 254 duty cycle, uptime averaged 3.3 minutes (out of the 4 minutes allocated), with a range of 2.8 – 3.8
 255 minutes due to variations in the start-up and shut-down time on each cycle.

256 3.3. Wave-powered Adaptable Monitoring Package (WAMP)

257 The WAMP was a first-of-a-kind integration of a sensor package with relatively high power
 258 requirements with a wave energy converter. This enabled continuous sensor operation and real-time
 259 processing, realizing many of the benefits of cabled deployments. Wave-generated power allowed
 260 us to maintain full operation of the AMP sensors for 84 % of the 3.5 month deployment: an order of
 261 magnitude increase in system activity relative to the AutoAMP for a deployment more than twice as
 262 long and with significantly higher power draw (Table 3). Data were transmitted back to shore over a
 263 high-bandwidth radio frequency link (>200 Mbps, Ubiquiti Networks Rocket 5AC Lite) that enabled
 264 review of collected data prior to system recovery and control of the AMP software. The AMP software
 265 was configured to archive data on a duty cycle (once every hour) or when targets were detected and
 266 tracked in the multibeam sonar data, using the same real-time processing module as for MSL-1.

267 The WAMP was deployed at the Wave Energy Test Site (WETS) in Kaneohe, HI (Figure 6). During
 268 the deployment, the average wave climate had a significant wave height of 1.9 m and energy period of
 269 8 s, with significant wave height increasing to 4.2 m during a storm. The WAMP was rigidly coupled
 270 to the wave energy converter (a BOLT-class Fred. Olsen Lifesaver), with the sensor head at a depth of 2
 271 m. This depth was selected as a trade-off between high cantilever loads on the mounting structure
 272 and a desire to avoid interference in the optical and active acoustic data from air bubbles. Joslin et
 273 al. [31] presents a complete discussion of structural design, power systems integration, and system
 274 performance. While this deployment demonstrated the potential for wave-generated power to enable

⁹ Hardware triggering to enable concurrent operation of all active acoustic instruments was implemented for the MSL-2 deployment.

275 environmental monitoring, the primary deployment motivation was to characterize marine animal
 276 interactions with the Fred. Olsen Lifesaver. This particular wave energy converter, with an outer
 277 diameter of 16 m, was capable of generating an order of magnitude more power than required for the
 278 WAMP. Smaller wave energy converters designed to power oceanographic observations are an area of
 279 active research and development (e.g., [32]).

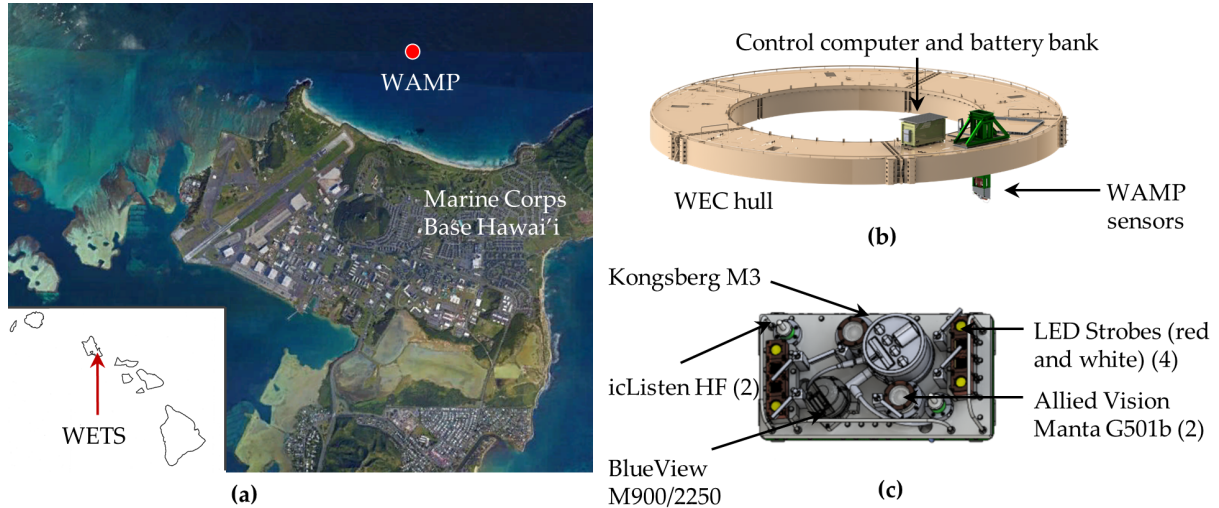


Figure 6. WAMP deployment showing (a) site layout, (b) AMP configuration, excluding power take-off modules on the Fred. Olsen Lifesaver, and (c) AMP sensors.

280 **3.4. MSL-2 Demonstration**

281 The final AMP deployment described here was in Sequim, WA (PNNL MSL), approximately 100
 282 m further into the channel than the first deployment (Figure 7), with peak currents ≈ 2 m/s. This
 283 system relied on real-time processing modules, primarily acquiring data when targets were detected
 284 and tracked in the multibeam sonar data and, secondarily, on a sparse duty cycle. Real-time target
 285 detection and classification capabilities were demonstrated [23].

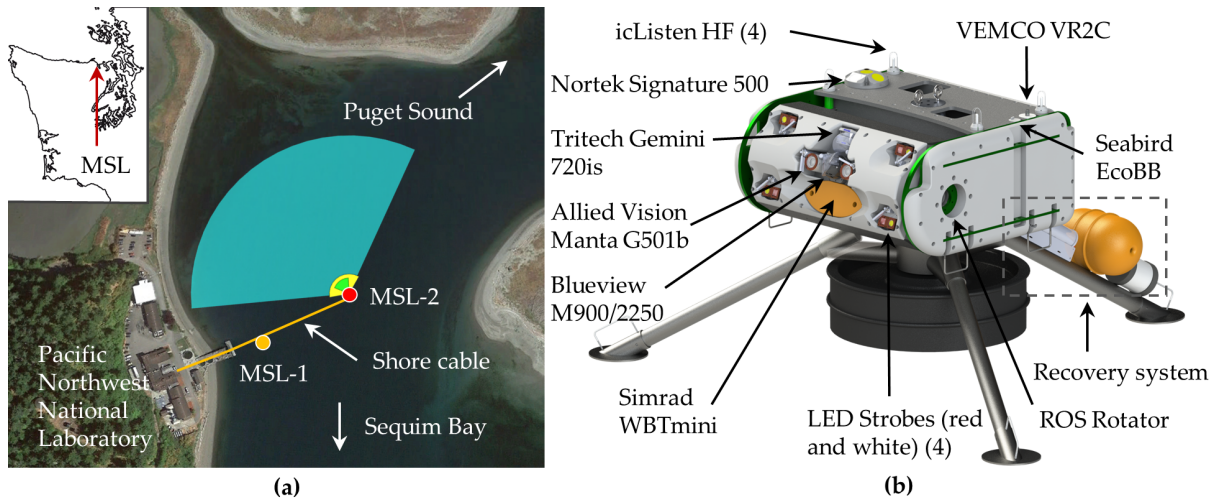


Figure 7. MSL-2 deployment showing (a) site layout and (b) AMP configuration.

286 **4. Results**

287 Here, we discuss trends across the four representative deployments in Section 3 with an emphasis
 288 on practical considerations, such as biofouling and corrosion, sensor performance across environments

289 and deployment modes, and the effectiveness of automated detection and classification algorithms
290 that can reduce the volume of data produced by continuous observation.

291 4.1. Practical Considerations

292 4.1.1. Biofouling and Mitigation

293 Figure 8 shows the condition of all four deployments at time of recovery, annotated with sensor
294 position and protective measures. Fouling varies strongly with location, depth, duration, and season.
295 For example, MSL-1 occurred entirely before seasonal barnacle recruitment in 2017, but MSL-2 was in
296 the water during recruitment and was recovered a month after barnacles began to grow. An earlier
297 deployment in 2016 was fouled similarly to MSL-2 and motivated the inclusion of UV lights in the
298 MSL-2 build to prevent barnacle colonization of the multibeam sonar transducers. The AutoAMP
299 had accumulated virtually no fouling at recovery and the WAMP, while in the water for longest, was
300 less fouled than MSL-2. Consequently, depending on deployment specifics and mitigation measures,
301 biofouling may either necessitate recovery after several months or be incidental to maintenance cycles.

302 In terms of mitigation measure effectiveness, mechanical wipers and copper face plates maintained
303 high optical clarity during all deployments. UV illumination for the MSL-2 deployment partially
304 prevented fouling on active sonars (Figure 8d), but multiple UV sources would be required to fully
305 illuminate the transducers, as shadowed areas accumulated significant fouling. We also note that
306 the echosounder, which was coated with zinc oxide paste prior to deployment, experienced limited
307 fouling. Similar treatment may be effective for multibeam transducers if deployment durations are
308 limited.

309 One type of “biofouling” we did not anticipate was reef effects. For the WAMP deployment, the
310 optical field of view was often “cluttered” by reef fish (dominantly sergeant majors, *Abudefduf saxatilis*)
311 (Figure 11b). Crabs also caused issues during two deployments. During MSL-1, a crab occupied the
312 interior cavity of the BlueView sonar for several days and generated a large number of automatic
313 detections that archived data without targets of interest. During the AutoAMP deployment, crabs
314 colonized the lander and the scraping of their carapaces on the metal surfaces periodically dominated
315 the soundscape at frequencies up to 1 kHz. Similar soundscape contributions at higher frequencies
316 have been documented for hermit crabs on coral reefs [33].

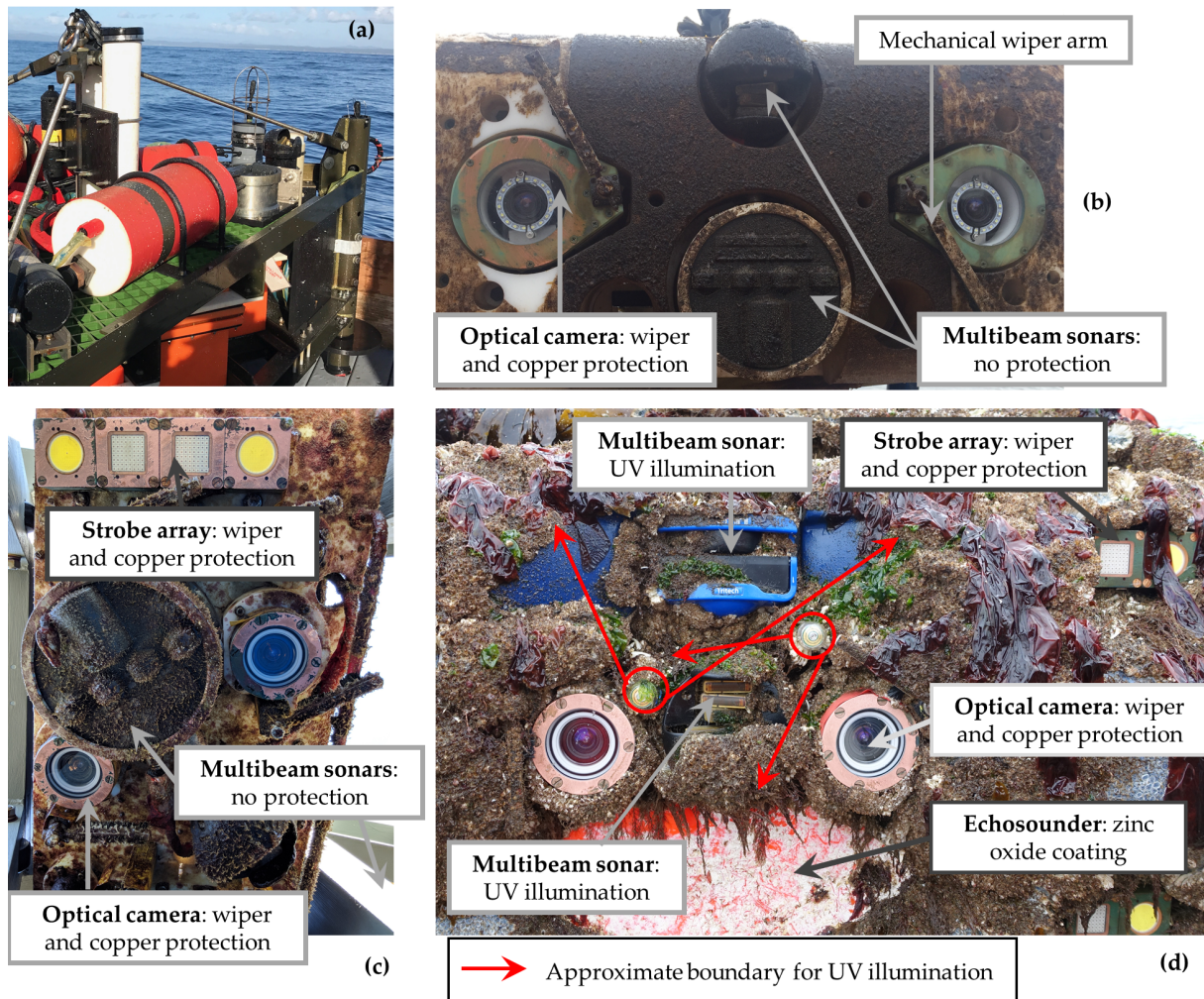


Figure 8. AMP biofouling at recovery for the four deployment case studies: (a) AutoAMP: 44 day at 70 m – negligible fouling, (b) MSL-1: 77 days at 8 m depth – limited fouling, (c) WAMP: > 200 days (system in water longer than operated) at 2 m depth – moderate fouling, and (d) MSL-2: 118 days at 7 m depth – heavy fouling.

317 4.1.2. Corrosion

318 We ensured that all systems were electrically isolated (Section 2.2), which limited instances
 319 of corrosion during all deployments. However, significant corrosion did occur at dissimilar metal
 320 interfaces on some manufacturer’s instruments, such as 316 stainless steel – titanium interfaces at
 321 bulkheads. Mild steel snap rings applied to these bulkheads were moderately effective at limiting
 322 corrosion rates, but complete mitigation would require a redesign by equipment manufacturers. We
 323 note that using zinc-alloy anodes to mitigate dissimilar metal corrosion between stainless steel and
 324 titanium is not recommended due to the large difference in anodic index¹⁰ [34].

325 4.1.3. Adjustable Field of View

326 While the inclusion of a tilt motor for the sensor head adds cost and complexity, our experience
 327 from MSL-2 is that these considerations are outweighed by increased functionality. First, the tilt motor
 328 allowed us to periodically look at the seabed to confirm sensor and illumination operation, as well as

¹⁰ A large anodic index will cause rapid wasting of the anode, such that the base metal can be unprotected for a substantial portion of a longer deployment.

329 observe gravel and shell hash movement in high currents. Second, after deployment, the tilt motor
 330 allowed us to optimally position the active acoustic sensors to minimize interference from the water
 331 surface and seafloor. Third, when we conducted testing around the AMP with cooperative targets, we
 332 were able to orient the sensors towards the surface to determine when a vessel was directly over the
 333 platform.

334 4.2. Sensor Performance

335 4.2.1. Optical Cameras

336 As shown in Figure 9, optical data can help communicate findings from an acoustic image,
 337 particularly at close range where it can be difficult to classify targets using sonar [23]. Overall, optical
 338 camera imagery can be used for species-level classification, is more easily interpreted than sonar data,
 339 and is more robust to platform motion.

340 The effective range of optical cameras is strongly site specific. At WETS, visibility greater than
 341 10 m was common and, in strong sunlight, the seabed was visible at a range of 30 m. In comparison,
 342 visibility at MSL was generally less than 5 m. At night, even with artificial illumination, range was
 343 reduced to a few meters at MSL and WETS. Depending on the size of marine energy converters, this
 344 range limitation can be a significant challenge for optical observations of interactions (Section 5.2).

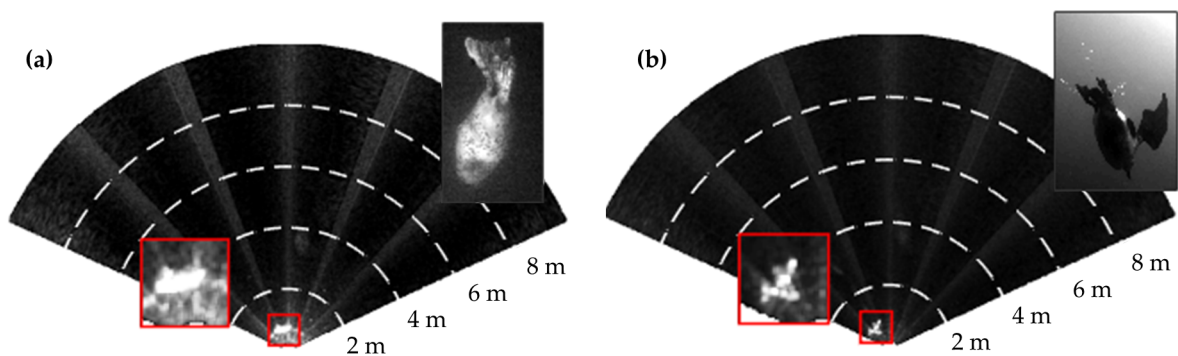


Figure 9. Comparison of optical and active acoustic (BlueView multibeam sonar, 2250 kHz) representations of a (a) seal and (b) diving bird from MSL-1. Adapted from [19].

345 4.2.2. Multibeam Sonars

346 The functional range of multibeam sonars was significantly greater than the optical cameras, but
 347 subject to interference from the seafloor or water surface depending on the position of the sonar in
 348 the water column. In a horizontal configuration (MSL-1 and MSL-2), target detection became more
 349 difficult once the sonar swath intersected the water surface or seabed.

350 During the WAMP deployment, when the multibeam sonars were positioned near the surface
 351 and oriented at an angle downwards towards one of the mooring lines, air bubbles in the upper water
 352 column caused two issues. First, even in calm sea states, air bubbles severely reduced the range of the
 353 BlueView's 2250 kHz transducer, requiring us to switch to the 900 kHz transducer. Second, air bubbles
 354 from breaking waves periodically obscured portions of the sonar swath (Figure 10a,b). The degree of
 355 obstruction increased in proportion to wave steepness (Figure 10c).

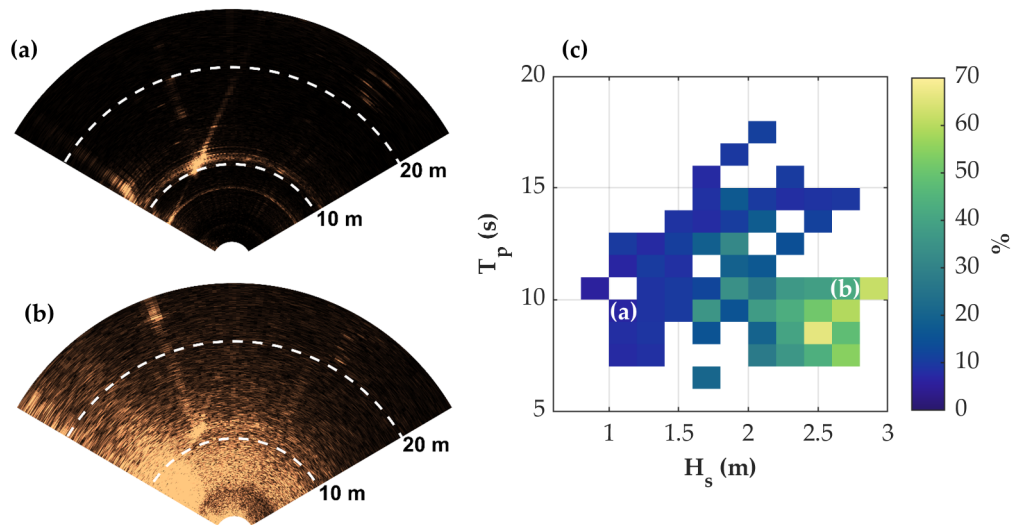


Figure 10. Kongsberg M3 multibeam sonar during WAMP deployment with (a) low and (b) high levels of bubble intrusion. (c) Average percentage of the sonar image (Kongsberg M3) that was obscured by bubbles as a function of the significant wave height (H_s) and peak wave period (T_p), based on an analysis of 147 sonar sequences. Sea states for (a) and (b) are annotated. The obstructed region was determined by applying a threshold to the image, and finding the region of the image above the threshold connected to the surface (e.g., left-hand side of (a)). Morphological filters (dilation and fill) were then applied to reduce the effects of noise.

356 4.2.3. Passive Acoustics

357 To date, passive acoustics on the AMP have primarily provided useful diagnostic information
 358 (e.g., correlating artifacts in sonar imagery with vessel wakes). At MSL, there are few vocalizing marine
 359 mammals and while humpback whales (*Megaptera novaeangliae*) are seasonally abundant at WETS,
 360 none were vocalizing during the WAMP deployment.

361 The localizing performance of the hydrophone array was quantified using “cooperative” targets
 362 (Vemco fish tags, Ocean Sonics icTalk HF transducer). During MSL-1, this testing revealed that the AMP
 363 body (Figure 4) significantly shadowed sound propagation to some of the hydrophones, depending on
 364 source position. This contributed to the redesign of the array for MSL-2 (Figure 7), which achieved
 365 more uniform performance in cooperative target testing. Similar interference occurred for the fish tag
 366 receiver placement on the AutoAMP (Figure 5). This was corrected for MSL-2 and, during in-situ tests,
 367 the receiver integrated with the AMP had a similar detection range to an autonomous fish tag receiver
 368 on a stand-alone mooring.

369 In general, passive-acoustic integration poses a design conflict between the need for hydrophones
 370 to be unobstructed (to avoid shadowing) and widely spaced (for accurate bearing estimation), and
 371 for instrumentation systems to be compact for ease of deployment and recovery. In addition to our
 372 experience with the AMP, in one recent tidal turbine deployment, hydrophone nodes were dispersed
 373 on a turbine’s support structure, which provided sufficient baseline separation for source localization.
 374 However, even with redundant hydrophones at each node, instrumentation failures rendered portions
 375 of the array inoperable, as the elements could not be serviced without recovering the entire turbine
 376 [35].

377 4.3. Automatic Target Detection and Classification

378 An outcome of hardware and software integration is the ability to work with multiple data
 379 streams in real time. This can enable continuous observation without accruing unmanageable volumes
 380 of data, as well as control sensors to minimize animal bias. As an example, if the AMP sensors for

MSL-2 (Table 2 and 3) were to continuously archive data, 1.2 TB of storage would be required per day, or ≈ 0.5 PB of storage per year. Automatic, real-time target detection that avoids archiving “empty” data can greatly reduce these storage requirements. Further reductions are possible with real-time target classification if not all targets in the field of view are of equal interest for an environmental monitoring study. For these reasons, automatic target detection and classification were implemented in real-time for multibeam sonar data for the MSL and WAMP deployments, and in post-processing for optical camera data. In this section, we summarize these efforts and some of the operational challenges encountered in their implementation. Full details of algorithm development and validation for the multibeam sonar are provided in separate publications [19,23].

4.3.1. Multibeam Sonar

For multibeam sonar processing, we emphasize that target detection (i.e., determining that a target is present in the sonar field of view) is independent from target classification (i.e., assigning a class to a detected target). Algorithms developed to date have been primarily applied to imagery from the BlueView M900-2250, but initial explorations suggest these results are transferable to the Tritech Gemini [24] and may be similarly transferable to the Kongsberg M3.

The real-time detection module first implemented during MSL-1 triggered data archival when targets were present in the multibeam sonar data using manually-tuned thresholds for apparent size and intensity. While this method produced a relatively high number of false positives (i.e., > 40 % of data acquisition triggers were caused by “non-biological targets”, such as sonar artifacts or high-intensity backscatter attributed to entrained air), it reduced the volume of data by an order of magnitude relative to continuous archiving [19]. To quantify detector accuracy, we reviewed nearly 1000 sequences when a data acquisition command was *not* generated by the detection module (e.g., no target was predicted to be present) and acquisition occurred on a regular duty cycle. Only 1 % of these sequences contained a target that was not automatically detected, which is an acceptable false negative rate. We also simulated duty cycle data collection and estimated that a 5 % duty cycle (45 seconds of data every 15 minutes) would be expected to capture just 6 % of the automatically detected events, and less than 2 % of recorded sonar sequences would contain a target of interest [19]. This means that duty cycle observation is unlikely to capture targets of interest that are infrequently present (i.e., “rare events”).

Target detection for the WAMP deployment proved more challenging because a mooring line and subsea float in the field of view created moving artifacts of comparable apparent size and intensity to biological targets of interest. This meant that target detection based on size and intensity thresholds was ineffective because thresholds that admitted biological targets would also admit most artifacts. We attempted to compensate for this by masking regions of the swath, but because the sonar motion was independent of float motion, the artifacts varied in apparent size, position, and intensity. Preliminary investigation suggests that the algorithm used for optical camera processing (Section 4.3.2) may be an effective alternative target detector for sonar imagery acquired from stationary and moving platforms and will be tested in future AMP deployments.

This detection step also facilitated the training of machine learning algorithms for automatic target classification. By reviewing only sequences with detected targets, relatively limited human effort was required to annotate the data to train machine learning algorithms for classification, as compared to annotating continuously acquired data. In post-processing, a random forest algorithm discriminated between biological (e.g., seals, schools of fish, and diving birds) and non-biological targets with a recall rate¹¹ of 0.97 and precision¹² of 0.60 [23]. Further, this algorithm was able to distinguish targets associated with seals, birds, and fish schools with recall rates of 0.91, 0.88, and 0.91,

¹¹ True positive classifications relative to actual members of the target class.

¹² True positive classifications relative to all positive classifications.

426 respectively. The inputs to the classification model are an optimized set of hand-engineered features
427 that describe statistical attributes of all detections making up a target's track (e.g., 75th percentile major
428 axis length) and environmental covariates (e.g., time of day) [23].

429 These training data were used to evaluate classification model performance and implement
430 real-time, automatic classification for MSL-2 [23]. Initially, when the classification model used for
431 MSL-2 was trained only using data collected at MSL-1, the model performed relatively poorly – less
432 than 50 % of biological targets were correctly classified (recall rates for biological target classes < 0.5)
433 [23]. This reduction in performance relative to recall rates of ≈ 0.9 in post-processing of MSL-1 data
434 is attributable to differences in site characteristics and biological activity between MSL-1 and MSL-2.
435 Specifically, the stronger currents at MSL-2 produced more non-biological targets associated with
436 entrained air. Similarly, at MSL-1, temporal patterns of biological activity were, in retrospect, affected
437 by artificial lighting on shore¹³. However, after a relatively small volume of new training data from
438 MSL-2 was added to the classification model, performance improved significantly, with greater than
439 70 % of biological targets correctly classified (recall rates for biological classes > 0.7). The site-specific
440 nature of biological classification algorithms trained with smaller volumes of data agrees with the
441 findings of Rosa et al. [36] for classification of birds in radar data.

442 4.3.2. Optical Cameras

443 Optical processing methods implemented to date involve concurrent target detection and
444 classification using the YOLO (You Only Look Once) deep-learning algorithm [37,38]. Our motivation
445 for using this algorithm stems from prior demonstrated success using this approach to detect fish in
446 optical imagery [39]. The YOLO algorithm produces both class identification and bounding box target
447 location in candidate images. Using a binary (i.e., biological vs. non-biological) YOLO model with
448 annotated imagery from MSL and WETS, we were able to obtain recall of 0.83 and precision of 0.96 in
449 WETS data when predicted bounding boxes had a 0.4 overlap divided by area (i.e., Intersection over
450 Union) threshold measured against ground truth data. Additionally, a two-class model to distinguish
451 reef fish (e.g., sergeant majors) from non-reef fish (e.g., a tuna-like species) produced a recall of 0.71
452 and precision of 0.96, averaged over the two classes, using the same evaluation criteria. To develop this
453 model, we employed an iterative process of training the model with limited data, then curating the
454 output and retraining with the expanded image set. At the end of this iterative process, we had curated
455 17,481 training images from MSL (primarily without targets present) and 2,469 training images from
456 WETS. In addition, automatic stereo image processing shows promise in extracting target size and
457 speed (Figure 11). To estimate target size, we: 1) extract YOLO-produced bounding boxes; 2) predict
458 corresponding targets between stereo images by searching for a similarly-sized bounding box along a
459 rectified image epipolar line [40], and; 3) triangulate the 3D bounding box corner positions using the
460 calibrated stereo extrinsics [41]. Similarly, to estimate target speed, we search temporally identified
461 YOLO bounding boxes for similarly sized-targets, and estimate speed as distance traveled divided by
462 time between captured frames. As target motion is not constrained, correspondence between temporal
463 frames cannot be limited to an epipolar line search, which makes accurate temporal correspondence
464 more difficult. As such, speed estimates have a relatively high implicit uncertainty, particularly when
465 multiple targets are present.

¹³ Harbor seals appeared primarily at night during MSL-1, likely because they were using the dock lighting to forage, but appeared throughout the day during MSL-2.

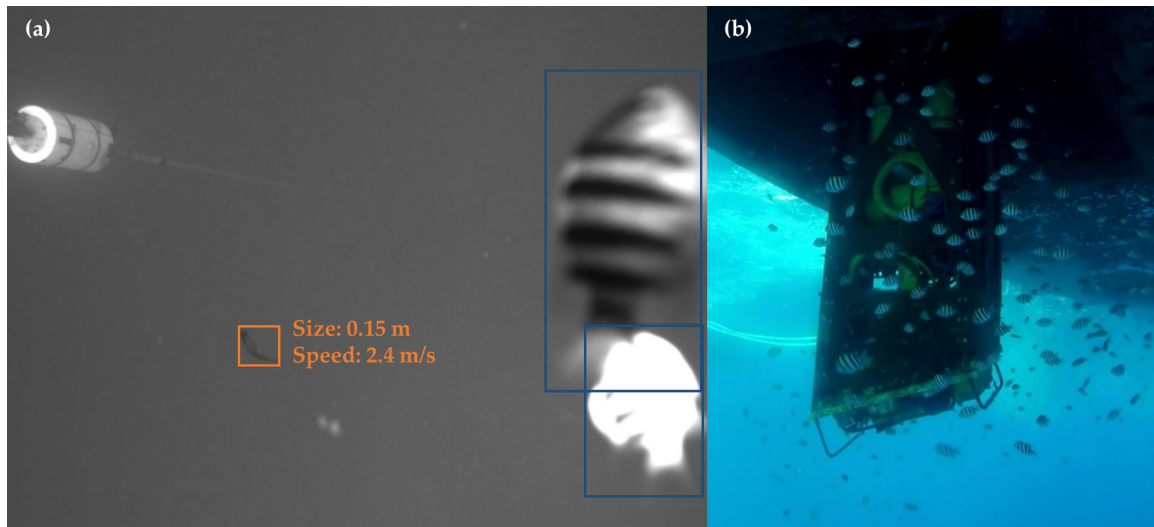


Figure 11. (a) Automated size and speed estimation from WAMP deployment imagery. Size is reported as the diagonal length of predicted 3D bounding box. The reef fish on the right margin have been automatically identified as not of interest. (b) Representative reef clutter observed by external camera during WAMP inspection.

466 5. Discussion

467 5.1. Evidenced Requirements for Integrated Instrumentation

468 Our experiences with AMP deployments evidence a number of requirements for effective use
 469 of integrated instrumentation systems at marine energy sites. First, to observe “rare events” without
 470 producing unmanageable volumes of data, it is essential to provide sufficient power for continuous
 471 sensor operation and real-time processing [19], whether by cable or in-situ energy harvesting. When
 472 limited by batteries, as for the AutoAMP (Section 3.2), the type of sensors that can be supported and
 473 the maximum allowable duty cycle are relatively low, given power requirements for sensing and
 474 real-time processing (Tables 2 and 3). As another example, the initial deployments of the FLOWBEC
 475 platform relied on battery power [12], which limited deployments to 14 days, restricted the sensor
 476 suite, did not allow real time data processing, and devoted the majority of the platform structure to
 477 battery storage.

478 Second, deployment outcomes are improved by providing connectivity for continuous data
 479 transmission. By reviewing data products in near real-time, problems can be rapidly identified and
 480 corrected, rather than only becoming apparent during a post-deployment analysis phase. For example,
 481 during the WAMP deployment, we initially enabled the 2250 kHz head on the BlueView sonar based
 482 on our favorable experience during MSL-1 and AutoAMP deployments. If we had not been able to
 483 review data during the WAMP deployment, we would not have discovered that air bubbles rendered
 484 it mostly ineffective until after recovery. The ability to access and review data at the time of collection
 485 also minimizes the risk of inadvertently accruing and curating large volumes of irrelevant data, as
 486 well as providing the opportunity for iterative model training (c.f., Section 4.3.2).

487 Third, integrated instrumentation should be designed to be maintained at intervals no longer than
 488 six months. Although no critical sensor failures have occurred during AMP deployments, problems
 489 such as corrosion at dissimilar metal interfaces on manufacturer-supplied equipment have been
 490 developed over our longest deployments. While it is likely that engineering solutions and biofouling
 491 mitigation measures can extend endurance beyond what we have demonstrated, we believe it is critical
 492 to design integrated instrumentation systems for recovery and repair.

493 5.2. Operational Concepts for Integrated Instrumentation

494 When integrated instrumentation is used to monitor marine energy installations, there are
495 multiple deployment options, all of which involve trade-offs. The first two evidenced requirements for
496 integrated instrumentation (power availability and data connectivity) are most easily satisfied by a
497 cabled connection to terrestrial facilities. Consequently, satisfying the third evidenced requirement
498 (maintenance intervention) suggests operational strategies that share a number of features with
499 maintenance of grid-connected marine energy converters (MECs). Specifically, if the instrumentation
500 is connected to a cable, then either the cable needs to be recovered along with the instrumentation or
501 a “docking” capability is required to connect to and disconnect from the cable. Similarly, there are
502 two approaches to securing the instrumentation package: integrating it into the structure of a MEC or
503 using a separate structure.

504 Operational concepts for integrated instrumentation can be classified by three attributes:

- 505 • *Securement strategy*: integrated with a MEC and independent structure;
- 506 • *Position in the water column*: surface, mid-water, and seabed; and
- 507 • *Marine energy resource*: waves, oscillating tidal currents, and continuous ocean currents.

508 The securement strategy restricts the range of stand-off distances between the integrated
509 instrumentation package and a MEC. Specifically, if the securement strategy is to integrate the
510 instrumentation with a MEC, then the *maximum* stand-off distance between the sensors and components
511 of interest on the MEC is likely on the order of 10 m, given the size of existing MECs. Conversely, if
512 an independent structure is used, then the *minimum* stand-off distance is likely on the order of 10 m
513 due to space requirements for marine operations to install and maintain the independent structure,
514 regardless of the position of the structure in the water column.

515 If a monitoring objective is to observe interactions between marine animals and a MEC, then
516 integrating instrumentation with a MEC is preferred. Our experience suggests that automatic
517 classification of targets in multibeam sonars becomes increasingly difficult at ranges greater than 10 m.
518 Similarly, outside of tropical waters, the range of optical cameras is generally less than 10 m. Given this,
519 the field of view will likely only include a portion of most utility-scale MECs. While sonar deployment
520 from an independent platform at greater stand-off distance may place an entire MEC within the
521 field of view [12], this arrangement significantly reduces image resolution, such that detection and
522 classification of smaller targets would be more difficult. In addition, moored, independent platforms
523 add data processing complexity due to relative motion and operational complexity due to the need to
524 control position and orientation during deployment.

525 The position in the water column imposes a number of restrictions for docking instrumentation
526 to a cabled node or recovering the cable. For surface deployments, docking or cable recovery is
527 relatively straightforward as the “docking” connection and cable handling can occur out of the
528 water (c.f., the WAMP). For subsurface deployments, docking and cable recovery have different
529 challenges. For docking, wet-mate power and data connections with sufficient bandwidth for
530 integrated instrumentation can be costly and the mating process often requires relatively fine alignment
531 and moderate engagement force¹⁴. Early AMP developments included successful demonstration of
532 a wet-mate system using an inspection-class ROV (Figure 12), and docking station [42,43], but the
533 complexity, risk, and cost motivated a cable recovery strategy for MSL-1 and MSL-2. For cable recovery,
534 the connectors can be dry-mate, with substantially lower cost, but this requires a customized approach
535 to controlling package orientation during redeployment, maintenance operations put the cable and
536 instrumentation system at risk, and steps must be taken to avoid collision or entanglement with a
537 nearby MEC. For the MSL deployments, the water was shallow enough for us to coarsely orient the
538 AMP with guy lines as it was deployed, but this would not be feasible in deeper water.

¹⁴ For example, a Teledyne ODI NRH connector can only tolerate a linear offset < 4 mm and an angular offset < 10° during mating and requires > 500 N engagement force.

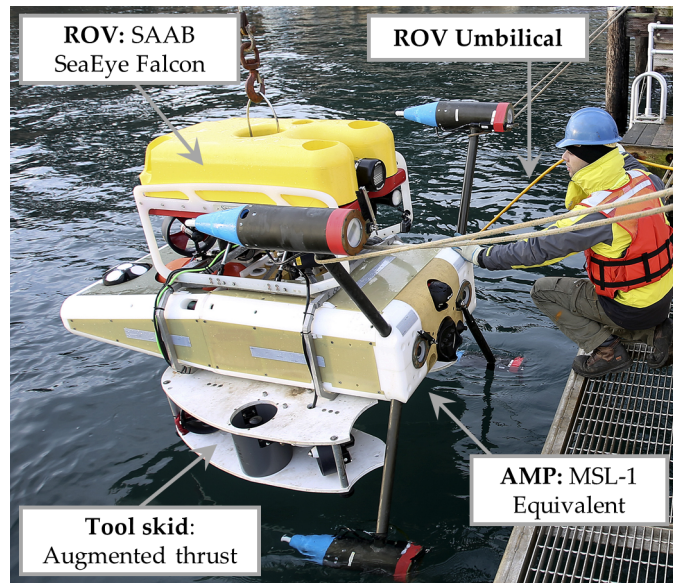


Figure 12. ROV deployable version of AMP tested prior to MSL-1. The ROV delivered the AMP to a pre-placed, cabled docking station (frame in Figure 4), engaged a wet-mate power and fiber connector (Teledyne ODI NRH), and then returned to the surface.

539 General operation and maintenance considerations for each resource type, depending on position
 540 in the water column and securement strategy, are summarized in Table 4. In doing so, we have
 541 assumed a nominal “mid-water” depth of 25 m and a nominal seabed depth of 50 m for tidal and
 542 wave energy, and a nominal seabed depth of 300 m for ocean current energy [5]. Each combination is
 543 assigned a qualitative difficulty denoted by the color shading, which progresses from relative ease
 544 (no shading) to operations that are infeasible with existing technology (dark blue). There are several
 545 apparent trends. First, there are no scenarios in which both operation and maintenance can be achieved
 546 with relative ease. Second, there is a trade-off between the simplicity of operations and the simplicity
 547 of maintenance. Third, wave energy installations are the most straightforward to instrument, followed
 548 by tidal currents. Ocean currents present a number of significant technical challenges for sub-surface
 549 instrumentation maintenance. Overall, operations and maintenance considerations should be central
 550 to instrumentation development and, optimally, a “co-design” exercise between those engaged in
 551 environmental monitoring and those deploying MECs.

552 We note that these capability concepts can be facilitated by complimentary technology
 553 developments. For example, non-contact power and data transfer solutions are under development and
 554 could substantially simplify the complexity of docking operations by eliminating physical connectors.
 555 Similarly, reducing the sensor payload would reduce the size of instrumentation packages and facilitate
 556 deployment and recovery. This requires environmental studies to identify the minimum sensor set
 557 needed to answer a specific question, which will likely only become apparent as questions are answered
 558 using a broader set of sensors.

559 5.3. Cost-Benefit of Integration

560 Instrument integration into a compact package is a difficult task. The successful demonstrations
 561 of AMP systems have had to overcome interference between active sonars, electrical noise on shared
 562 power busses¹⁵, Ethernet traffic conflicts, and the need to rewrite instrument control and data
 563 acquisition software. This raises the question of whether integration is worthwhile.

¹⁵ As an example, the load on the primary Vicor DC-DC power converters in the integration hub (Table 1) had a measureable effect on the noise floor for the WBTmini echosounder, even though the power busses were nominally independent. Specifically, in passive mode, the WBTmini noise floor varied by more 14 dB, based on which instruments were energized,

Table 4. Generalized operation and maintenance considerations wave wave, tidal and ocean current systems. Color progression from light to dark denotes difficulty. For waves, if water depth decreases (50 m nominal), wave orbital velocities are appreciable over relatively more of the water column. For oscillatory tidal currents, if water depth decreases (50 m nominal), currents near the seabed and at mid-water converge towards surface values. For continuous ocean currents, the region of significant currents extends to > 50 m depth.

Environment	Instrument Location	Operations		Maintenance	
		Integrated with MEC	Independent Platform	Integrated with MEC	Independent Platform
Waves	Surface (<2 m)	<ul style="list-style-type: none"> High structural loads on sensors Significant platform motion possible Air bubbles occlude field of view 	<ul style="list-style-type: none"> Air-side access to sensors 	<ul style="list-style-type: none"> Air-side access to cable 	
	Mid-water (25 m)	<ul style="list-style-type: none"> Moderate structural loads and limited platform motion 	<ul style="list-style-type: none"> ROV or diver intervention 	<ul style="list-style-type: none"> Heavy lift capacity to raise platform and cable to surface^a 	
	Seabed (50 m)	<ul style="list-style-type: none"> Low structural loads and no platform motion 	<ul style="list-style-type: none"> ROV intervention 	<ul style="list-style-type: none"> Moderate lift capacity to raise platform and cable to surface 	
Oscillatory Tidal Currents	Surface (< 2 m)	<ul style="list-style-type: none"> Highest structural loads: strongest currents at surface Air bubbles occlude field of view 	<ul style="list-style-type: none"> Air-side access to sensors 	<ul style="list-style-type: none"> Air-side access to cable 	
	Mid-water (< 2 m)	<ul style="list-style-type: none"> Moderate structural loads: currents decrease with depth 	<ul style="list-style-type: none"> ROV or diver intervention during slack water 	<ul style="list-style-type: none"> Heavy lift capacity to raise platform and cable to surface during slack water 	
	Seabed (50 m)	<ul style="list-style-type: none"> Lowest structural loads: currents at minimum near seabed 	<ul style="list-style-type: none"> ROV intervention during slack water 	<ul style="list-style-type: none"> Heavy lift capacity to raise platform and cable to surface during slack water 	
Continuous Ocean Currents	Surface (<2 m)	<ul style="list-style-type: none"> Highest structural loads: strongest currents at surface Air bubbles occlude field of view 	<ul style="list-style-type: none"> Air-side access to sensors 	<ul style="list-style-type: none"> Air-side access to cable 	
	Upper water column (50 m)	<ul style="list-style-type: none"> Moderate structural loads: currents decrease with depth 	<ul style="list-style-type: none"> High-thrust ROV required 	<ul style="list-style-type: none"> Heavy lift capacity vessel with high thrust required 	
	Seabed (300 m)	<ul style="list-style-type: none"> Stand-off between sensors and turbine exceeds sensor range 	<ul style="list-style-type: none"> ROV with launch and recovery system^b 	<ul style="list-style-type: none"> Heavy lift capacity vessel with high thrust required 	

^a A mid-water platform in waves would likely have more significant mooring and anchoring requirements than a platform on the seabed and, therefore, require heavier lift capability for recovery.)

^b To overcome drag in upper water column

564 One way to think about integration is in terms of “phases”, with each phase enabling a
 565 fundamental capability. We define Phase 1 integration as providing power and data connectivity
 566 to a range of sensors through a common backbone. This enables hardware deployment as a single,
 567 integrated package. Phase 2 integration involves a common software architecture for sensor control
 568 and data acquisition. This enables synchronous and duty-cycled data acquisition. Phase 3 integration
 569 builds on this by evaluating data streams in real time to make decisions about data acquisition and
 570 sensor control.

571 In our opinion, there are clear benefits to each phase, but the cost-benefit trade-off may not
 572 always favor integration. Phase 1 integration dramatically simplifies maintenance. Further, if a
 573 MEC-integrated strategy is employed (Section 5.2), the interface specification for an integrated package
 574 on a turbine or wave energy converter can be as simple as a bolt pattern and a cable for power and
 575 data. Distributing instrumentation across a wider area can have benefits for passive acoustic tracking
 576 [35] and stand-off distance, but significantly increases integration cost and precludes the evidenced
 577 requirement for independent maintenance of sub-surface instrumentation. Phase 1 integration also
 578 allows multiple fields of view to be observed from a single platform and make concurrent observations
 579 of marine animals with different sensing modalities (Figure 9, Figure 13). Overall, our experience is
 580 that the benefits of Phase 1 integration outweigh the costs.

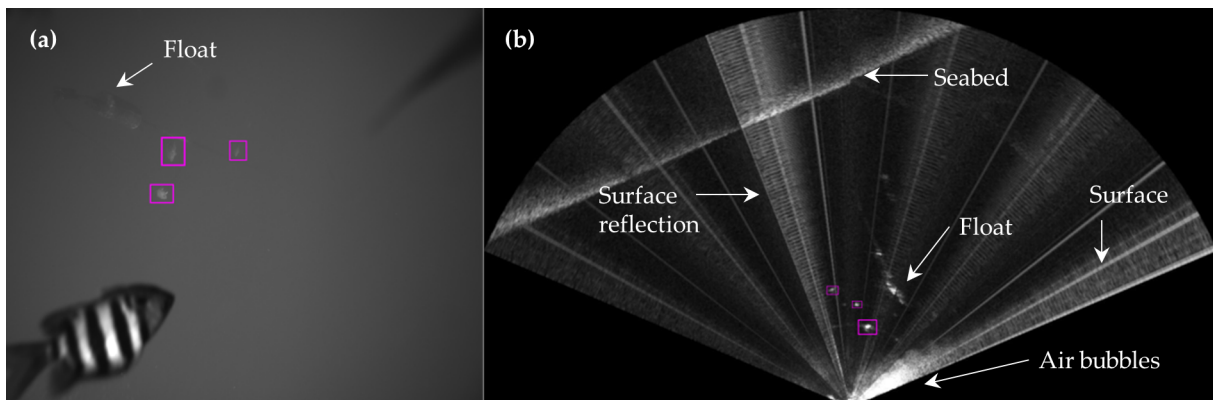


Figure 13. (a) Three fish automatically detected by the YOLO optical algorithm (outlined in magenta) also apparent in (b) BlueView multibeam sonar data (manually outlined in magenta).

581 Phase 2 integration requires setting aside much of the software written by manufacturers and
 582 rebuilding functionality using manufacturer-provided software development kits or communication
 583 protocol specifications. It would be difficult to overstate the difficulty we encountered in this process.
 584 While Phase 2 integration does simplify duty-cycle acquisition and guarantees that all acquisition
 585 occurs on the same master clock (though does not preclude master clock drift without a cabled
 586 connection or GPS), it could be argued that the cost to achieve this is disproportionate to the benefits.
 587 In general, outside of stereo image processing, precise timing is not critical – knowing that an animal
 588 was present with sub-second accuracy is not likely much more informative than knowing it was
 589 present within a 10-second period.

590 However, Phase 2 integration is a precursor to Phase 3 integration, which, in our experience, is
 591 the only way to address the prioritized monitoring requirements laid out in Section 1 and resolve
 592 the implicit conflict between the priorities. In addition to reducing data volumes from continuous
 593 observation (Section 4.3), when data are evaluated in real time, the risk of behavioral bias associated
 594 with some observations can be substantially mitigated. For example, decisions can be made about
 595 enabling artificial illumination for optical acquisition based on target proximity, as determined

including mechanical wipers and UV lights. This change in noise floor has the effect of reducing the echosounder’s operational range and signal-to-noise ratio.

596 from a multibeam sonar. Phase 3 integration also provides real-time classification models access
597 to environmental correlates, such as water current velocity and direction. In our opinion, the greatest
598 benefits from Phase 3 integration are the ones that have yet to be realized, as the marine biology
599 community should be able to use integrated architectures to conduct new types of targeted observation
600 (e.g., long-term predator-prey interaction studies). This could also enable machine learning already
601 employed in oceanographic studies (e.g., [44]) to be utilized in real time. Similarly, integrated
602 instrumentation has clear applications to port and harbor security and, perhaps, other applications yet
603 to be considered.

604 6. Conclusions

605 In this paper, we have presented details of the AMP system, described system and sensor
606 performance across four, multi-month deployments, and demonstrated the feasibility of integrated
607 instrumentation in cabled and autonomous modes of operation. Our experience with AMP
608 development is that an integrated instrumentation system can provide a reliable and cost-effective
609 solution to environmental monitoring at marine energy sites. However, we emphasize that significant
610 non-recurring engineering effort is required to develop such systems and, consequently, this should
611 not be undertaken lightly. System design must consider the specific environmental questions to be
612 studied, as well as considerations for operation and maintenance in marine energy environments (e.g.,
613 biofouling mitigation, deployment strategy). Full integration of hardware and software allows rare
614 events to be observed, minimizes the volume of data not containing interactions of interest, avoids
615 biasing animal behavior while sensing, and enables tractable maintenance strategies. Concurrent
616 developments in marine energy and integration instrumentation have implications beyond our ability
617 to monitor environmental interactions for utility-scale marine energy converters. As demonstrated by
618 the WAMP deployment, coupling integrated instrumentation with small wave energy converters or
619 current turbines can enable observations similar to a cabled observatory – but without the cable. While
620 hardware and software challenges undoubtedly remain, integrated instrumentation systems like the
621 AMP have reached a point of maturity where they can effectively contribute to the body of knowledge
622 about the environmental effects of marine energy.

623 **Author Contributions:** Conceptualization, B.P., J.J., A.S., and E.C.; methodology, B.P., J.J., A.S., E.C., P.M., and C.B.;
624 software, E.C., P.M., and M.S.; formal analysis, E.C. and M.S.; investigation, J.J., P.M., P.G., E.C., and M.S.; data
625 curation, E.C., P.M., and M.S.; writing–original draft preparation, B.P., J.J., E.C., P.G., P.M., M.S.; writing–review and
626 editing, C.B. and A.S.; visualization, P.G., E.C., M.S., B.P., and J.J.; supervision, B.P. and A.S.; project administration,
627 B.P. and A.S.;

628 **Funding:** This material is based upon work supported by the U.S. Department of Energy’s Office of
629 Energy Efficiency and Renewable Energy (EERE) under the Water Power Technologies Office award numbers
630 DE-EE0006788 and DE-EE0007827. The WAMP deployment was supported by the U.S. Department of Defense’s
631 Naval Facilities Engineering Command (N00024-08-D-6323 Task Order No. 16). E.C. was supported by a National
632 Science Foundation Graduate Research Fellowship.

633 **Acknowledgments:** The authors would like to acknowledge the technical contributions of the following
634 individuals and organizations:

- 635 • *University of Washington:* Haleh Bahadori, Eric Boget, Robert Cavagnaro, Corey Crisp, Jesse Doshier, Bryan
636 Ford, Craig Hill, John Horne, Trina Litchendorf, Ben Maurer, Darshan Mehta, Jessica Noe, Andy Reay-Ellers,
637 Chris Siani, Zack Tully, and Benjamin Williamson;
- 638 • *Oregon State University:* Sarah Henkel, Geoff Hollinger, and the crew of R/V Pacific Storm;
- 639 • *Pacific Northwest National Laboratory:* Kate Hall, Geneva Harker-Klimes, Kailan Mackereth, Margaret Pinza,
640 Shari Matzner, Sue Southard, Garrett Staines, and John Vavrinc;
- 641 • *University of Hawai’i:* Patrick Cross and Andrew Druetzler;
- 642 • *Sea Engineering, Inc.:* Patrick Anderson and Andrew Rocheleau; and
- 643 • *Fred. Olsen Renewables:* Even Hjetland.

644 **Conflicts of Interest:** J.J. is commercializing the AMP technology through MarineSitu, Inc. The funders had no
645 role in the design of the study; in the collection, analyses, or interpretation of data; in the writing of the manuscript,
646 or in the decision to publish the results.

647 Abbreviations

648 The following abbreviations are used in this manuscript:

649

3D	Three-dimensional
AMP	Adaptable Monitoring Package
API	Application Programming Interface
AutoAMP	Autonomous AMP
DC	Direct Current
650 MSL	Marine Science Laboratory
PNNL	Pacific Northwest National Laboratory
ROV	Remotely Operated Vehicle
SDK	Software Development Kit
WAMP	Wave-powered AMP
WETS	Wave Energy Test Site

651 References

- 652 1. Copping, A.; Sather, N.; Hanna, L.; Whiting, J.; Zydlewski, G.; Staines, G.; Gill, A.; Hutchison, I.; O'Hagan,
653 A.; Simas, T.; others. Annex IV 2016 state of the science report: Environmental effects of marine renewable
654 energy development around the world. Technical report, International Energy Agency Ocean Energy
655 Systems, 2016.
- 656 2. Copping, A.; Hemery, L. OES-Environmental 2020 State of the Science Report: Environmental Effects
657 of Marine Renewable Energy Development Around the World. Technical report, International Energy
658 Agency Ocean Energy Systems, 2020.
- 659 3. Gunn, K.; Stock-Williams, C. Quantifying the global wave power resource. *Renewable Energy* **2012**,
660 *44*, 296–304.
- 661 4. Falnes, J.; Kurniawan, A. *Ocean waves and oscillating systems: linear interactions including wave-energy
662 extraction*; Vol. 8, Cambridge university press, 2020.
- 663 5. Barnier, B.; Domina, A.; Gulev, S.; Molines, J.M.; Maitre, T.; Penduff, T.; Le Sommer, J.; Brasseur, P.; Brodeau,
664 L.; Colombo, P. Modelling the impact of flow-driven turbine power plants on great wind-driven ocean
665 currents and the assessment of their energy potential. *Nature Energy* **2020**, *5*, 240–249.
- 666 6. Karsten, R.; Swan, A.; Culina, J. Assessment of arrays of in-stream tidal turbines in the Bay of
667 Fundy. *Philosophical Transactions of the Royal Society A: Mathematical, Physical and Engineering Sciences*
668 **2013**, *371*, 20120189.
- 669 7. Polagye, B.; Thomson, J. Tidal energy resource characterization: methodology and field study in Admiralty
670 Inlet, Puget Sound, WA (USA). *Proceedings of the Institution of Mechanical Engineers, Part A: Journal of Power
671 and Energy* **2013**, *227*, 352–367.
- 672 8. Lewis, M.; Neill, S.; Robins, P.; Hashemi, M. Resource assessment for future generations of tidal-stream
673 energy arrays. *Energy* **2015**, *83*, 403–415.
- 674 9. Bassett, C.; Thomson, J.; Polagye, B. Sediment-generated noise and bed stress in a tidal channel. *Journal of
675 Geophysical Research: Oceans* **2013**, *118*, 2249–2265.
- 676 10. Polagye, B.; Copping, A.; Suryan, R.; Kramer, S.; Brown-Saracino, J.; Smith, C. Instrumentation for
677 monitoring around marine renewable energy converters: Workshop final report. Technical Report
678 PNNL-23100, Pacific Northwest National Laboratory, Seattle, WA, USA, 2014.
- 679 11. Hasselman, D.; Barclay, D.; Cavagnaro, R.; Chandler, C.; Cotter, E.; Gillespie, D.; Hastie, G.; Horne, J.; Joslin,
680 J.; Long, C.; McGarry, L.; Mueller, R.; Sparling, C.; Williamson, B. Environmental Monitoring Technologies
681 and Techniques for Detecting Interactions of Marine Animals with Marine Renewable Energy Devices. In
682 *In A.E. Copping and L.G. Hemery (Eds.), OES-Environmental 2020 State of the Science Report: Environmental
683 Effects of Marine Renewable Energy Development Around the World*; International Energy Agency Ocean Energy
684 Systems, 220; pp. 177–212.
- 685 12. Williamson, B.J.; Blondel, P.; Armstrong, E.; Bell, P.S.; Hall, C.; Waggitt, J.J.; Scott, B.E. A self-contained
686 subsea platform for acoustic monitoring of the environment around Marine Renewable Energy
687 Devices—Field deployments at wave and tidal energy sites in Orkney, Scotland. *IEEE Journal of Oceanic
688 Engineering* **2015**, *41*, 67–81.

- 689 13. Hastie, G.D.; Gillespie, D.M.; Gordon, J.C.; Macaulay, J.D.; McConnell, B.J.; Sparling, C.E. Tracking
690 technologies for quantifying marine mammal interactions with tidal turbines: pitfalls and possibilities. In
691 *Marine Renewable Energy Technology and Environmental Interactions*; Springer, 2014; pp. 127–139.
- 692 14. Cotter, E.; Murphy, P.; Bassett, C.; Williamson, B.; Polagye, B. Acoustic characterization of sensors used for
693 marine environmental monitoring. *Marine pollution bulletin* **2019**, *144*, 205–215.
- 694 15. Marchesan, M.; Spoto, M.; Verginella, L.; Ferrero, E.A. Behavioural effects of artificial light on fish species
695 of commercial interest. *Fisheries research* **2005**, *73*, 171–185.
- 696 16. Widder, E.; Robison, B.; Reisenbichler, K.; Haddock, S. Using red light for in situ observations of deep-sea
697 fishes. *Deep Sea Research Part I: Oceanographic Research Papers* **2005**, *52*, 2077–2085.
- 698 17. Wiesebron, L.E.; Horne, J.K.; Hendrix, A.N. Characterizing biological impacts at marine renewable energy
699 sites. *International Journal of Marine Energy* **2016**, *14*, 27–40.
- 700 18. Wilding, T.A.; Gill, A.B.; Boon, A.; Sheehan, E.; Dauvin, J.C.; Pezy, J.P.; O'beirn, F.; Janas, U.; Rostin, L.;
701 De Mesel, I. Turning off the DRIP ('Data-rich, information-poor')—rationalising monitoring with a focus on
702 marine renewable energy developments and the benthos. *Renewable and Sustainable Energy Reviews* **2017**,
703 *74*, 848–859.
- 704 19. Cotter, E.; Murphy, P.; Polagye, B. Benchmarking sensor fusion capabilities of an integrated instrumentation
705 package. *International journal of marine energy* **2017**, *20*, 64–79.
- 706 20. Cowles, T.; Delaney, J.; Orcutt, J.; Weller, R. The ocean observatories initiative: Sustained ocean observing
707 across a range of spatial scales. *Marine Technology Society Journal* **2010**, *44*, 54–64.
- 708 21. Hayes, S.; Mangum, L.; Picaut, J.; Sumi, A.; Takeuchi, K. TOGA-TAO: A moored array for real-time
709 measurements in the tropical Pacific Ocean. *Bulletin of the American Meteorological Society* **1991**, *72*, 339–347.
- 710 22. Kohler, P.C.; LeBlanc, L.; Elliott, J. SCOOP-NDBC's new ocean observing system. OCEANS 2015-MTS/IEEE
711 Washington. IEEE, 2015, pp. 1–5.
- 712 23. Cotter, E.; Polagye, B. Automatic classification of biological targets in a tidal channel using a multibeam
713 sonar. *Journal of Atmospheric and Oceanic Technology* **2020**.
- 714 24. Cotter, E.; Polagye, B. Biological detection and classification capabilities of two multibeam sonars. *Limnology*
715 *and Oceanography Methods* **In revision**.
- 716 25. Demer, D.; Andersen, L.; Bassett, C.; Berger, L.; Chu, D.; Condiotty, J.; Cutter, G. Evaluation of a wideband
717 echosounder for fisheries and marine ecosystem science. Technical Report 336, ICES Cooperative Research
718 Report, 2017.
- 719 26. Watkins, W.A.; Schevill, W.E. Sound source location by arrival-times on a non-rigid three-dimensional
720 hydrophone array. *Deep Sea Research and Oceanographic Abstracts* **1972**, *19*, 691 – 706.
721 doi:[https://doi.org/10.1016/0011-7471\(72\)90061-7](https://doi.org/10.1016/0011-7471(72)90061-7).
- 722 27. Wahlberg, M.; Møhl, B.; Teglberg Madsen, P. Estimating source position accuracy of a large-aperture
723 hydrophone array for bioacoustics. *The Journal of the Acoustical Society of America* **2001**, *109*, 397–406.
- 724 28. Jaffe, J.S. Underwater optical imaging: the design of optimal systems. *Oceanography* **1988**, *1*, 40–41.
- 725 29. Joslin, J.; Polagye, B.; Parker-Stetter, S. Development of a stereo-optical camera system for monitoring tidal
726 turbines. *Journal of Applied Remote Sensing* **2014**, *8*, 083633.
- 727 30. Joslin, J.; Polagye, B. Demonstration of biofouling mitigation methods for long-term deployments of optical
728 cameras. *Marine Technology Society Journal* **2015**, *49*, 88–96.
- 729 31. Joslin, J.B.; Cotter, E.D.; Murphy, P.G.; Gibbs, P.J.; Cavagnaro, R.J.; Crisp, C.R.; Stewart, A.R.; Polagye, B.;
730 Cross, P.S.; Hjetland, E.; Rocheleua, A.; Waters, B. The wave-powered adaptable monitoring package:
731 hardware design, installation, and deployment. Proceedings of the 13th European Wave and Tidal Energy
732 Conference; Vicinanza, D., Ed., 2019.
- 733 32. Mundon, T.R. Performance evaluation and analysis of a micro-scale wave energy system. Proceedings of the
734 13th European Wave and Tidal Energy Conference; Vicinanza, D., Ed.; EWTEC, , 2019; pp. 1686–1–1686–8.
- 735 33. Freeman, S.E.; Rohwer, F.L.; D'Spain, G.L.; Friedlander, A.M.; Gregg, A.K.; Sandin, S.A.; Buckingham, M.J.
736 The origins of ambient biological sound from coral reef ecosystems in the Line Islands archipelago. *The*
737 *Journal of the Acoustical Society of America* **2014**, *135*, 1775–1788.
- 738 34. Roberge, P.R. *Handbook of corrosion engineering*; McGraw-Hill, 2000.
- 739 35. Malinka, C.E.; Gillespie, D.M.; Macaulay, J.D.; Joy, R.; Sparling, C.E. First in situ passive acoustic monitoring
740 for marine mammals during operation of a tidal turbine in Ramsey Sound, Wales. *Marine Ecology Progress*
741 *Series* **2018**, *590*, 247–266.

- 742 36. D. Rosa, I.M.; Marques, A.T.; Palminha, G.; Costa, H.; Mascarenhas, M.; Fonseca, C.; Bernardino, J.
743 Classification success of six machine learning algorithms in radar ornithology. *Ibis* **2016**, *158*, 28–42.
- 744 37. Redmon, J.; Divvala, S.; Girshick, R.; Farhadi, A. You only look once: Unified, real-time object detection.
745 Proceedings of the IEEE conference on computer vision and pattern recognition, 2016, pp. 779–788.
- 746 38. Redmon, J.; Farhadi, A. Yolov3: An incremental improvement. *arXiv preprint arXiv:1804.02767* **2018**.
- 747 39. Xu, W.; Matzner, S. Underwater fish detection using deep learning for water power applications. 2018
748 International Conference on Computational Science and Computational Intelligence (CSCI). IEEE, 2018,
749 pp. 313–318.
- 750 40. Papadimitriou, D.V.; Dennis, T.J. Epipolar line estimation and rectification for stereo image pairs. *IEEE*
751 *transactions on image processing* **1996**, *5*, 672–676.
- 752 41. Hartley, R.I.; Sturm, P. Triangulation. *Computer vision and image understanding* **1997**, *68*, 146–157.
- 753 42. Rush, B.; Joslin, J.; Stewart, A.; Polagye, B. Development of an Adaptable Monitoring Package for marine
754 renewable energy projects Part I: Conceptual design and operation. Proceedings of the 2nd Marine Energy
755 Technology Symposium, 2014.
- 756 43. Joslin, J.; Polagye, B.; Rush, B.; Stewart, A. Development of an adaptable monitoring package for marine
757 renewable energy projects Part II: hydrodynamic performance. Proceedings of the 2nd Marine Energy
758 Technology Symposium, 2014.
- 759 44. Sheehan, E.V.; Bridger, D.; Nancollas, S.J.; Pittman, S.J. PelagiCam: a novel underwater imaging system
760 with computer vision for semi-automated monitoring of mobile marine fauna at offshore structures.
761 *Environmental Monitoring and Assessment* **2020**, *192*, 11.

762 © 2020 by the authors. Submitted to *J. Mar. Sci. Eng.* for possible open access
763 publication under the terms and conditions of the Creative Commons Attribution (CC BY) license
764 (<http://creativecommons.org/licenses/by/4.0/>).